1661-8726/09/020223-23
DOI 10.1007/s00015-009-1313-5
Birkhäuser Verlag, Basel, 2009

Swiss J. Geosci. 102 (2009) 223–245

Alpine tectonic evolution and thermal water circulations of the Argentera Massif (South-Western Alps)

Alessandro Baietto [1], P. Perello [2], P. Cadoppi [1] & G. Martinotti [1]

Key words: Argentera Massif, tectonic evolution, kinematic analysis, transpressive and extensional tectonics, hydrothermal circulations, buoyancy-driven flow

ABSTRACT

Three groups of thermal springs with temperatures close to 70 °C discharge both in the core (at Bagni di Vinadio and Terme di Valdieri) and on the external margin (at Berthemont-Les-Bains) of the Argentera Massif. Detailed structural field analysis carried out on the hydrothermal sites allows us to delineate both a model of Alpine tectonic evolution of the Argentera Massif and the patterns of hydrothermal circulation that were active during its final exhumation. The observed fault rock assemblages provide information relative to deformation that occurred in viscous, frictional-to-viscous and frictional crustal regimes. During the Early Miocene, the Bersezio Fault Zone and the Fremamorta Shear Zone, two main mylonitic shear zones, mainly accommodated regional transpression and provided pathways for fluid flow promoting mineral reactions in greenschist facies. During the Late Miocene–Early Pliocene, frictional-to-viscous deformation affected the massif, which underwent predominant transpression in the internal sectors and extension on the external margin. During the Plio-Pleistocene, deformation in frictional condition accompanied the final exhumation of the massif in a transpressive regime and resulted in the development of the NW–SE striking cataclastic zones. The hydraulic properties of these structures mainly influence the patterns of the active thermal circulations and the localization of the recharge and discharge zones. At Berthemont these faults represent conduits, whereas at Vinadio and Valdieri they form complex systems of conduits and barriers. In these two latter sites, the cataclastic faults compose flower structures that constrain laterally the thermal fluid flows while intensely fractured granites sited at depth constitute a highly-transmissive geothermal reservoir. Less permeable migmatitic gneisses overlaying the granites prevent a massive infiltration of the cold fluids at depth. This context favours within the high-permeability fractures granites the development of buoyancy-driven flows which combined with topographically-driven flows, provided the conditions for the upflow of the high-temperature waters.

1. Introduction

The Central and Western Alps display widespread evidence of past and present thermal circulations, whose activity is controlled by permeable fault systems. Notably, the past activity is testified by the occurrence of ore deposits, while the present activity is mainly represented by low-enthalpy thermal springs and water inflows in deep tunnels, with flow rates of 0.1–50 kg/s and temperatures of 20–70 °C (Vuataz 1982; Rybach 1995). The origin of the present-day thermal systems of the Alps relies on deep (>1 km) groundwater circulations in areas of normal or slightly higher than normal geothermal gradient, rather than on cooling of igneous bodies as in other classical geothermal sites, e.g. Larderello, Italy (Dallmeyer & Liotta 1998); Cerro Prieto, Mexico (Quintanilla & Suarez 1996); Long Valley Caldera, USA (Sanders et al. 1995) and Taupo Volcanic Zone, New Zealand (Rowland & Sibson 2004). In spite of the abundant information on the chemical and isotopic composition of the thermal waters (Martinotti et al. 1999; Pastorelli et al. 1999; Marini et al. 2000; Pastorelli et al. 2001), only a few studies focussed on the lithological and tectonic constraints controlling their localization in the structural Alpine framework. As an example, Perello (1997) pointed out that the geographical distribution of some thermal outflows suggests a likely control by important late-Alpine (Neogene) brittle shear zones. Many thermal water discharges (ca. ten groups) are located close to the Penninic Front, being a ductile deformation zone, reactivated by brittle shearing during the late Neogene (Laubscher 1991; Hubbard & Mancktelow 1992; Seward & Mancktelow 1994; Perello et al. 2001).

The Argentera Massif (AM) is one of the zones of the Western Alps with the highest concentration of thermal activity related to the occurrence of fault systems. The AM represents a pre-Triassic crystalline slice of thickened crust cropping out at the footwall of the Penninic Thrust (Fig. 1). In pre-Alpine and Alpine times, the massif underwent ductile to brittle deformational histories that culminated with the final exhumation of

[1] DST, Dipartimento di Scienze della Terra, Università di Torino, Via Valperga Caluso 35, 10125, Torino, Italy. E-mail: alessandro.baietto@unito.it
[2] SEA Consulting Srl, Via Cernaia 27, 10121, Torino, Italy.

the massif that occurred during the Pliocene (Bogdanoff et al. 2000; Bigot-Cormier et al. 2000). Within the AM, three main groups of thermal springs that have been known since the Roman period discharge at the margins of regional NW-trending strike-slip fault zones. The spring sites are known as *Bagni di Vinadio* (I), *Terme di Valdieri* (I) and *Berthemont-Les-Bains* (F). The Bagni di Vinadio and Terme di Valdieri discharges are located in the AM core, about 17 km apart (Perello et al. 2001), while the Berthemont-Les-Bains springs are located in the south-western part of the massif, close to the contact with the Dauphiné-Helvetic covers (Romain 1985; Fig. 2). The maximum outlet temperatures are close to 70 °C (Vinadio and Valdieri) and to 30 °C (Berthemont). The waters have a pH of 8–9 and the total dissolved salts attain 2000 mg/l at Vinadio, 250 mg/l at Valdieri and 260 mg/l at Berthemont. All the waters share a meteoric origin (Fancelli & Nuti 1978; Michard et al. 1989) and, according to geothermometric determinations, the Vinadio and Valdieri waters attain reservoir temperatures close to 150 °C (Perello et al. 2001). All these groups of springs discharge on valley bottoms at the borders of NW-trending shear zones. Rock alteration phenomena and ore deposits occur along the faults located in proximity to the thermal outlets, indicating that these structures also acted in the past as conduits for thermal flows (Colomba 1904; Cevales 1961; Perello et al. 2001).

Although it is apparent that the faults involved in shearing during the last deformational phases of the AM also drive the final up-well of the thermal fluids to the surface, it still remains an open question where these fluids infiltrate and circulate, and which mechanisms account for the thermal outflow. Moreover, present-day tectonic and kinematic interpretations are sometimes contradictory and need to be integrated into a single multi-stage tectonic model. In fact, although there is a general agreement that from the Miocene onward the external crystalline massifs underwent outward thrusting driving their erosional denudation (Mugnier et al. 1990), contrasting deformational styles are documented in different parts of the AM. As an example, it has been proposed that during the Pliocene the central part of the massif experienced a transpressive deformation with the right-lateral shear of the NW-trending Bersezio Fault, cutting through all the massif, and the thrusting of the NE Argentera onto the rest of the massif along the E-trending Fremamorta Shear Zone (Bigot-Cormier et al. 2000; Tricart 2004; cfr. Fig. 2). Besides, Labaume et al. (1989) suggest that in the same period the northern part of the Bersezio fault zone could have been affected by normal faulting, and an extensional deformation was occurring on the northwestern part of the AM. Thus, in order to understand correctly the relationships between the fault systems and past and active hydrothermal circulations, it is first necessary to improve the knowledge of the tectonic mechanisms that were active in different parts of the massif during its progressive exhumation. This is possible since kinematic information relative to structures that are referable to different crustal levels are available and allow for the performance of separate analysis and interpretation.

This work provides a structural description of the Argentera fault systems in the sectors around the thermal discharges of Vinadio, Valdieri and Berthemont. Detailed field investigations allowed us to recognize structures that formed at different crustal levels and finally to reconstruct a model of tectonic evolution of the massif. These studies also shed new light on the hydraulic behaviour of the faults and on the mechanisms governing the past and present-day hydrothermal flows. With the increasing demand for the exploitation of renewable energy sources, knowing how and where the thermal circulations take place becomes crucially important.

2. Geologic and structural setting of the Argentera Massif

The Argentera Massif (French–Italian Alps), together with the other external crystalline massifs (ECM) of the Western Alps (Fig. 1), represents a slice of pre-Triassic basement cropping out in the footwall of the Penninic Frontal Thrust (Fig. 1). These massifs correspond to the thickened European upper crust located at the front of the metamorphic internal arc (e.g. Schmid et al. 2004 for review). The Argentera Massif (AM) is

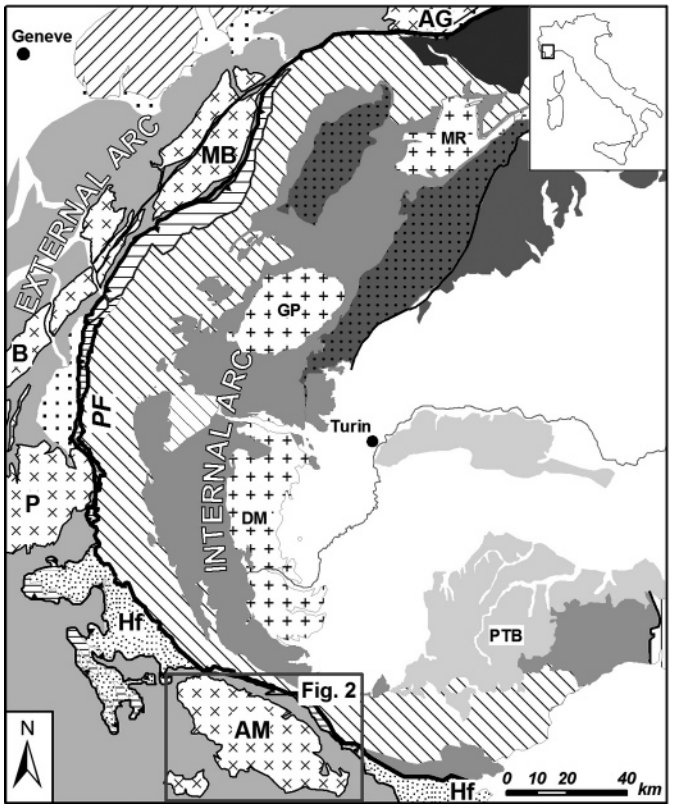

Fig. 1. Simplified tectonic map of the Central-Western Alps and adjacent regions, with location of the study area (in the inset). *External crystalline massifs*: AG – Aar-Gothard Massif, MB – Mont Blanc Massif, B – Belledonne Massif, P – Pelvoux Massif, AM – Argentera Massif. *Internal crystalline massifs*: MR – Monte Rosa Massif, GP – Gran Paradiso Massif, DM – Dora Maira Massif. PTB – Piedmont Tertiary Basin, Hf – Helmintoid Flysch. PF – Penninic Frontal Thrust. Modified after Structural Model of Italy (CNR, 1990).

the southernmost among the ECM and consists of high-grade metamorphic and intrusive rocks, unconformably covered by Triassic to Early Cretaceous carbonates that are mostly detached above the Late Triassic evaporites (Faure-Muret 1955; Malaroda et al. 1970).

The basement consists of two gneissic complexes, the Malinvern–Argentera Complex (MAC) and the Tinée Complex (TC), sited on the north-western and on the south-eastern part of the massif, respectively. The MAC is mainly constituted by migmatitic gneisses related to pre-Alpine, high-grade metamorphism of both para- and ortho-derivatives (Bogdanoff 1986). The migmatites are composed of quartz, K-feldspar, plagioclase, biotite and minor muscovite and sillimanite (Malaroda et al. 1970; Malaroda 1999). High-grade gneisses are intruded by syn-anatectic, leucocratic, granites and by calc-alkaline granites that emplaced at 293 ± 10 Ma (Ferrara & Malaroda 1969; Compagnoni et al. 1974). The TC is similar to the MAC in that it mainly consists of anatectic gneisses derived partly from sedimentary and from intrusive protoliths (Bogdanoff 1986). The migmatites are often interlayered with amphibolites, marbles, quartzites, graphitic schists and metadiorites. Both complexes experienced early eclogitic and granulitic metamorphisms followed by a syn-migmatitic event and late horizontal shearing (Latouche & Bogdanoff 1987). Rubatto et al. (2001) documented the occurrence of two distinct HP–HT events in the range 443–332 Ma and proposed an age of 323 Ma for the amphibolite facies metamorphism and anatexis, and an Upper Stephanian/Lower Permian age for the granites. Both the MAC and TC are overlaid by a sedimentary succession (Dauphiné–Helvetic cover), which is presently exposed around the basement. The cover can be subdivided into an autochthonous succession of Carboniferous–Triassic age and a detached succession of post-Late Triassic age (Faure-Muret 1955; Sturani 1962; Malaroda et al. 1970). Carboniferous–Permian sediments are of continental derivation, while Triassic–Oligocene succession mainly consists of dolostones, limestones, schists and meta-arenites (Faure-Muret 1955). Tertiary terrigenous sediments deposited from the Mid-Eocene to the Pliocene represent the remnants of the foreland basins that formed during Tertiary collision between the Apulian plate and the European passive margin. An internally-derived unit, the so-called Helminthoid Flysch, presently exposed north and south-east of the Argentera, was overthrusted on the foreland sequences starting from the Early Oligocene (Kerckhove 1969; Campredon & Giannerini 1997; Ford et al. 1999).

The structural setting of the AM is the result of late-Alpine brittle reactivations of networks of pre-Alpine and early-Alpine ductile shear zones, these latter deformed under greenschist facies conditions (Corsini et al. 2004). A main NW–SE shear zone, namely the Valletta Shear Zone (VSZ; Faure-Muret 1955; Bogdanoff 1986), also known as the Ferriere–Mollières Line (Malaroda *et al.* 1970), crosscuts the AM and separates the MAC from the TC (Fig. 2). The VSZ branches to the north in the Bersezio Fault (BF; Vernet 1965; Horrenberger et al. 1978), a NW–SE fault located close to the thermal site of Bagni di

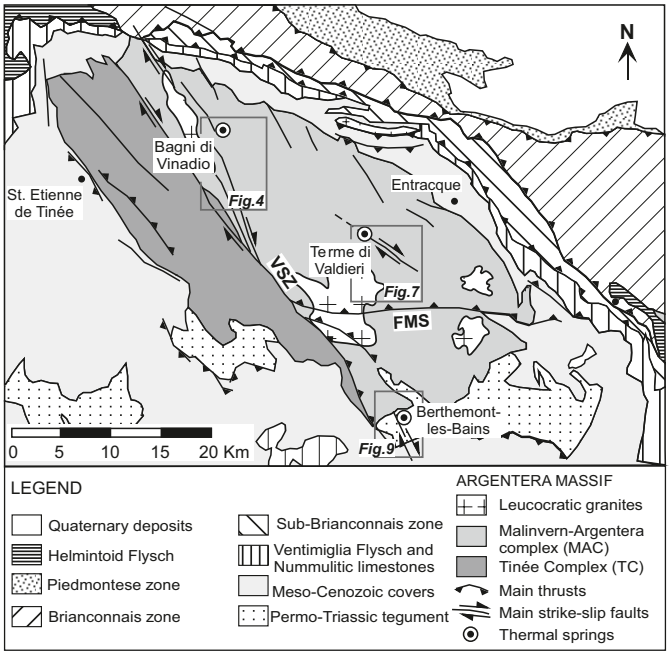

Fig. 2. Tectonic sketch map of the Argentera Massif and adjoining regions. Modified after Malaroda et al. (1970), Bogdanoff (1986), Structural Model of Italy (CNR, 1990), Perello (1997) and Larroque et al. (2001). BF – Bersezio Fault, VSZ – Valletta Shear Zone, FMS – Fremamorta Shear Zone, LF – Lorusa Fault. Hydrothermal springs discharge at the sites of Bagni di Vinadio (1300 m; I), Terme di Valdieri (1370 m; I), Berthemont-Les-Bains (1000 m; F).

Vinadio (Fig. 4). To the NE, the VSZ is constituted by up to 1 km-thick mylonitic rocks that formed during a pre-Alpine stage (Musumeci & Colombo 2002). These rocks, which were partly derived by ductile shearing of high-grade metamorphic rocks of both the TC and MAC (Bogdanoff 1986), have foliations striking NW–SE, steeply dipping toward SW and NE. In the central part of the massif, the VSZ connects with the Fremamorta Shear Zone (FMS), an important E–W oriented mylonitic corridor crosscutting the whole eastern part of the massif (Fig. 2). Along the FMS, the mylonitic foliation dips moderately to the north and the shear criteria indicate a reverse shear sense (Malaroda *et al.* 1970; Bogdanoff 1986). An indication that ductile shearing also occurred during an Alpine stage is provided by ^{39}Ar-^{40}Ar data on synkinematic phengites within the mylonites of the FMS (Corsini et al. 2004). According to these data, the ductile deformation occurred at ca. 22.5 Ma and the T–P estimates indicate 350 °C and 0.35–0.4 GPa, respectively, which would imply a minimum burial of 10–14 km (assuming gradients of 25–35 °C/km) for the AM. These depths may have corresponded to the phase of emplacement of the Helminthoid Flysch, a 3 to 4 km-thick nappe stack (based on metamorphic grade and fission track studies, Kerckhove 1969; Merle & Brun 1984; Seward et al. 1999), in the foreland basin after the Early Oligocene (at the most 28 Ma; Ford et al. 1999; Corsini et al. 2004). Therefore, the time range of 28–22.5 Ma could have corresponded to the major Alpine compressive event that culmi-

nated with the southward displacement of the tectonic pile of sediments (Labaume et al. 1989; Guardia et al. 1996; Laurent et al. 2000).

Most of the late-Alpine brittle deformation occurred through the reactivation of pre- and early- Alpine ductile shear zones (Perello et al. 2001). Zircon and apatite *FT* data of samples collected in the whole massif allowed Bigot-Cormier et al. (2000) to document the occurrence of different cooling histories and to propose that several tectonic blocks were subject to distinct vertical paths. According to zircon FT ages, the whole Argentera massif underwent a first cooling stage from 29 Ma, while a second cooling pulse occurred at ca. 22 Ma, with a rate approaching 1.3 mm/yr. This latter pulse is interpreted by Bigot-Cormier et al. (2000) in terms of an erosional denudation of the relief that was created by thrust tectonics during the Early Miocene. According to these authors, apatite FT indicates a cooling pulse at ca. 3.5 Ma, with exhumation rates of 1.1–1.4 mm/yr (assuming gradients of 30–25 °C/km, respectively). According to Bigot-Cormier et al. (2000), the VSZ acted at this age as a south-west-directed thrust that yielded a vertical offset of 500 m between the NE and SW part of the AM.

3. Descriptive criteria of the AM fault rocks

The new information produced in this work allows a better characterization of the shear zones previously described. Different assemblages of fault rocks with heterogeneous distribution and complex geometric relationships were recognized in the sectors of Vinadio, Valdieri and Berthemont. These are mainly constituted by: (1) mylonitic rocks, (2) quartz and chlorite fibres and aggregates coating slickensides and filling veins, (3) fault breccia and zones of intense fracturing and (4) layers of cataclasites and gouges. The deformational styles and the mineralogical assemblages associated with these fault rocks indicate the occurrence of Alpine deformational phases that were active under different crustal conditions. Using the fault rock classification proposed by Schmid & Handy (1991), these criteria allowed us to attribute the development of the Argentera fault rocks to

Viscous regime:	mylonites
Frictional-to-viscous transition regime:	quartz–chlorite slickensides and veins
Frictional regime:	cataclasites, gouges, fault breccia, fractured protolith rocks.

Mylonites (Fig. 3h) constitute the oldest fault rocks observed in the AM and their development can be ascribed to a viscous regime. The age of the mylonites is still a matter of debate. They were initially attributed by Malaroda et al. (1970) and by Musumeci & Colombo (2002) to pre-Alpine deformations and subsequent reworking during the Alpine phase. However, Corsini et al. (2004) recently interpreted some mylonites of the Argentera as the product of deformations under exclusive lower greenschist conditions that occurred at 22.5 Ma. In the internal parts of the AM, the lack of stratigraphic markers prevents a clear distinction between pre-Alpine and Alpine mylonites. However, the widespread occurrence of dynamic greenschist blastesis seems to indicate that most of the mylonites that are discussed in this work developed during an Alpine deformation phase.

The quartz–chlorite slickensides (abbreviated as qz–chl slickensides; Fig. 3f) here observed are attributed to a crustal level where a transition between the frictional and viscous regimes occurs. The growth fibres associated with these faults (Fig. 3g) are made up of quartz, chlorite and subordinate albite and epidote, indicating a lower-greenschist facies. Arrays of tension gashes filled with quartz and chlorite often occur close to the slickensides, and probably formed syn-kinematically. In proximity to the slickensides, the quartz–feldspathic mylonitic foliation of some mylonites is locally plastically dragged. The type of metamorphic facies and the occurrence of crystal plasticity next to the fault planes are two factors that, according to the criteria proposed by Schmid & Handy (1991), suggest a transition between a viscous and a frictional behaviour. In the continental crust, the frictional–viscous transition is generally believed to be located in the mid-crust (ca. 10–15 km depth) and to exist over a depth range of several kilometres (e.g. Snoke et al. 1998 and references therein). Slickensides crosscutting through Permian deposits are observed both in the internal and external parts of the massif, suggesting an Alpine age to this deformation. Unlike the cataclastic-gouge faults which compose pervasive high-strain zones, the slickensides are typically less pervasive although diffused across the examined sites. The local kinematic indications provided by measuring the fibre steps on slickensides are compared for various sectors and finally combined in order to reconstruct a kinematic model of the deformation that occurred in the frictional–viscous regime.

Fault rocks such as those indicated in the third category are generally believed to develop in the upper crust in a regime of frictional flow involving brittle fracture and dilatancy (Sibson 1977; Schmid & Handy 1991; Snoke et al. 1998). In the three examined sites, the cataclasites and gouges (Fig. 3a) occur in networks of multiple and interconnected layers, whereas the fault breccia (Fig. 3b) and fractured protoliths occur both in thick zones located on the external borders of the fault cores (Fig. 3d) and in lens-shaped blocks (Fig. 3c) enveloped by cataclastic-gouge layers. The cataclastic-gouge strands compose strike-slip faults with lengths of up to several kilometres (Fig. 3e).

In general, the attribution of the fault rocks development to different crustal regimes has undoubtedly a relative validity since, as it is widely acknowledged (e.g. Tullis & Yund 1977; Hirth & Tullis 1994; Holdsworth 2004), different processes can be active at similar depths depending on the local conditions (T, P, stress rate, etc.). However, the subdivision that is proposed here provides a useful preliminary procedure for separating

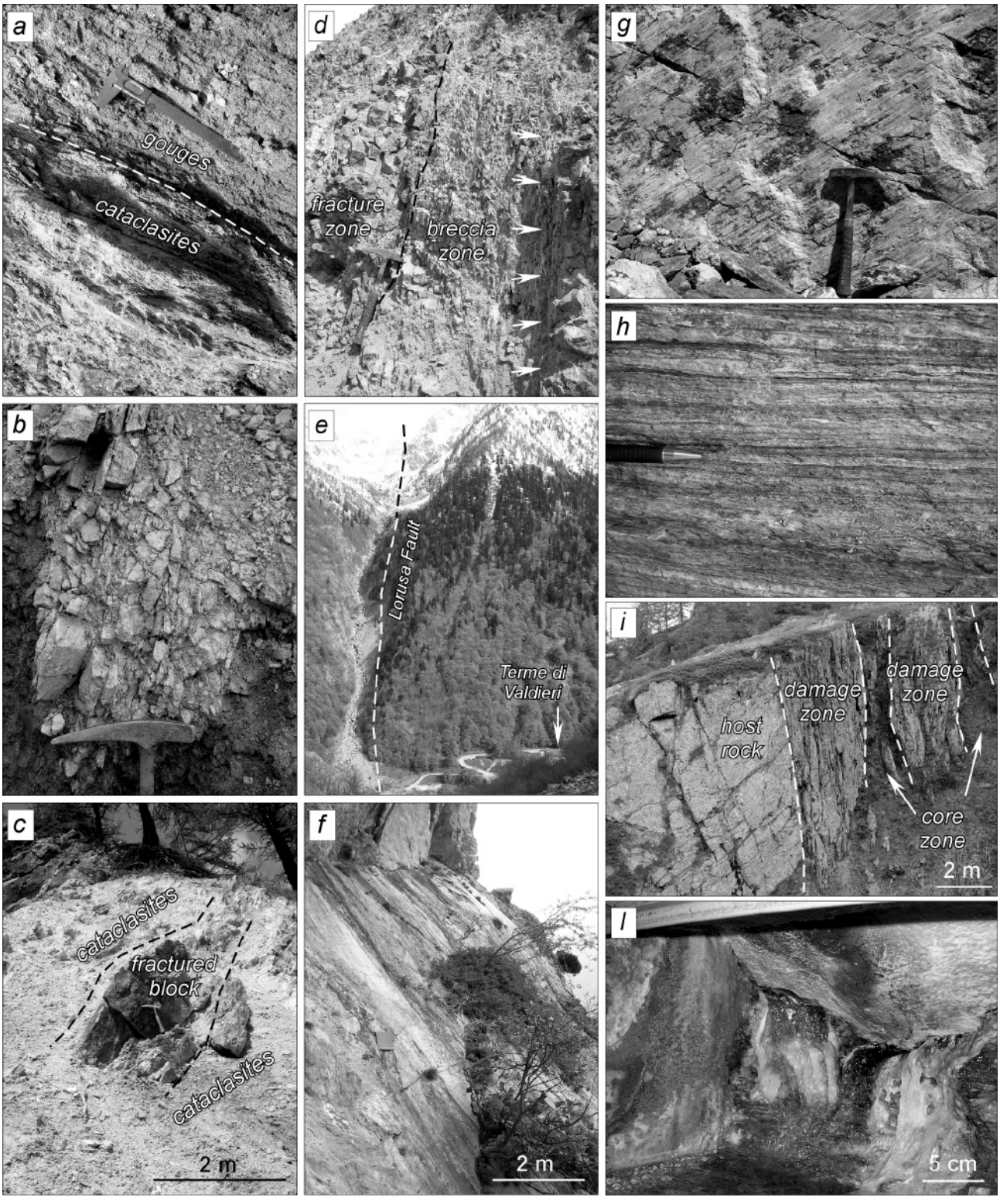

Fig. 3. Field images illustrating fault rocks of the AM. *Fault rocks relative to a frictional regime*: a) foliated cataclasites and gouges, b) fault breccia composed of cm-thick angular fragments, c) eye-shaped block of fractured migmatites wrapped by hydrothermally altered cataclasites, d) exposure of a fault damage zone composed of breccia and pervasively fractured migmatites (arrows indicate a cataclastic layer bounding the breccia), e) the Lorusa Fault at Terme di Valdieri; *Fault rocks relative to a frictional–viscous transition*: f) curvilinear slickenside coated by quartz–chlorite, g) slickenfibre of quartz and chlorite; *Fault rocks relative to a viscous regime*: h) mylonites in the migmatitic gneisses; i) boundaries between fractured host rocks, damage zones and core zones, l) hot spring discharging through a narrow fracture at Berthemont-Les-Bains.

information related to rocks that are likely to have formed at different crustal levels.

Following this criterion, geometric, kinematic and hydraulic fault data relative to different stages of the Argentera tectonic evolution are discussed separately for the sectors of Vinadio, Valdieri and Berthemont.

The deformation that occurred during the progressive exhumation of the AM was accompanied by episodes of hydrothermal flow. Different styles of deformation also produced different flow patterns. In particular, this work focusses on the hydraulic characters of the fault zones that developed in the frictional regime. The spatial distribution relative to the fault cores (i.e. the low permeability portion of a fault where most of the displacement is accommodated; e.g. Caine et al. 1996; Evans et al. 1997) and damage zones (i.e. the network of subsidiary structures that bound the fault core and with an enhanced permeability relative to the core and the undeformed protolith) of the main strike-slip faults is analysed (Fig. 3i). This allows us to reconstruct a scheme explaining how the past hydrothermal circulations, whose occurrence is testified by the hydrothermal alteration of fault zones and the active thermal fluid flows (Fig. 3l) have been influenced by the spatial distribution of structures with different hydraulic behaviours.

4. Structural characters of the thermal sectors

4.1. The Bagni di Vinadio sector

The Bagni di Vinadio thermal springs discharge at several sites through intensely fractured aplitic dykes located at the margins of a regional fault zone, here indicated as the Bersezio Fault Zone (BFZ). The label BFZ refers to a broad association of interlinked faults (Fig. 4a), also comprising structures such as the Bersezio Fault (BF) and the Valletta Shear Zone (VSZ), that were previously studied independently (Faure-Muret 1955; Malaroda et al. 1970; Bogdanoff 1986; Horrenberger et al. 1978). The BFZ is constituted by a ca. 3 km-wide high-strain belt, bounded to the NE by the BF and to the SW by the VSZ, this latter separating the Malinvern–Argentera Complex (MAC) from the Tinée Complex (TC). Widespread evidence of argillic rock alteration along several main fault strands of the BFZ attest to an intense thermal fluid flow that was also active in the past.

In this sector, migmatitic gneisses, fine-grained aplitic granites and minor slices of sedimentary rocks crop out. Small dykes of aplitic granites cutting the migmatitic foliation are widespread around Vinadio. Besides, the so-called St. Anna borehole (1895 m a.s.l.; Fig. 4a), which was drilled in the core of the BFZ, next to the St. Anna Sanctuary, down to a depth of 1150 m and at 60° north-eastward (Darcy 1997), reveals the occurrence of a thick granitic body beneath the migmatites at 850 m below the surface. The sedimentary rocks are found in a hundreds-of-metres-thick slice pinched within the TC migmatitic gneisses and cropping out below the Sespoul Peak (French side; cfr. Fig. 4a). The slice consists of yellow cavernous Triassic limestones, dolostones and strongly tectonized cargneules that have been affected by pervasive fluid leaching and carbonate precipitation. This structure has been previously interpreted as a thrusted syncline by Bogdanoff (1986), while more recently Baietto (2007) proposed that it could represent the result of a former graben fill that was subsequently reworked by a transpressive deformation.

A pervasive mylonitic foliation pre-dating the quartz–chlorite slickensides and cataclastic foliation occurs through the whole BFZ. Mylonitization affects zones up to tens of metres thick and is associated with a NW–SE striking foliation moderately dipping to the NE and to the SW (Fig. 4c). Mylonites characterized by greenschist mineralogical associations are widespread and occur in cm- to m-thick bands showing proto- to ultra-mylonitic fabrics. At the macro-scale, they compose anastomosing zones enveloping lithons of migmatites with preserved pre-Alpine fabrics. The mylonitic zones are mainly NW–SE to N–S striking and show S-C shear bands whose geometric arrangement is consistent with a right-lateral sense of shear. The pervasive chloritization and albitization along the mylonitic zones suggests that these zones acted as major conduits for regional fluid flow.

4.1.1. Frictional-to-viscous transition

Quartz–chlorite slickensides with lengths up to 10 m and widths of 1–5 cm are homogeneously distributed within the BFZ, inside the less deformed blocks bounded by the main cataclastic faults. Although the observed slickensides are typically very little pervasive, they are widespread over the area. These minor discrete faults are composed of sets of mutually interconnected shallowing- and steeply- dipping planes, which define "fault-stepped" (*sensu* Harland 1971) arrays. These features are also present as relics within the cataclastic zones, suggesting that the regions of cataclasis and fracturing were previously accommodating strain components (in a frictional to viscous regime), the intensity of which is difficult to evaluate due to the strong overprinting of the later structures.

Strikingly, several slickensides occurring in neighbouring regions display contrasting kinematic indications: some are characterized by combinations of wrench and contraction components, while others by wrench and extension strain components. At the macro-scale, the strain patterns indicating wrench–contraction and wrench–extension are accommodated in different sectors and, in turn, each of these components shows meso-scale partitioning. The sectors showing different structural associations were consistently distinguished into eleven domains (D1–11), hundreds of metres long and broadly elongate in the NW–SE direction (Fig. 5). D1–7 are wrench–contraction, D8–10 are wrench–extension and D11 is pure wrench-dominated. Although the boundary between adjacent domains is usually marked by main cataclastic faults, in some cases, the boundary of these structural domains is somewhat arbitrary. In all domains, it is apparent that no superposition between kinematically opposed structures has occurred, suggesting that a process

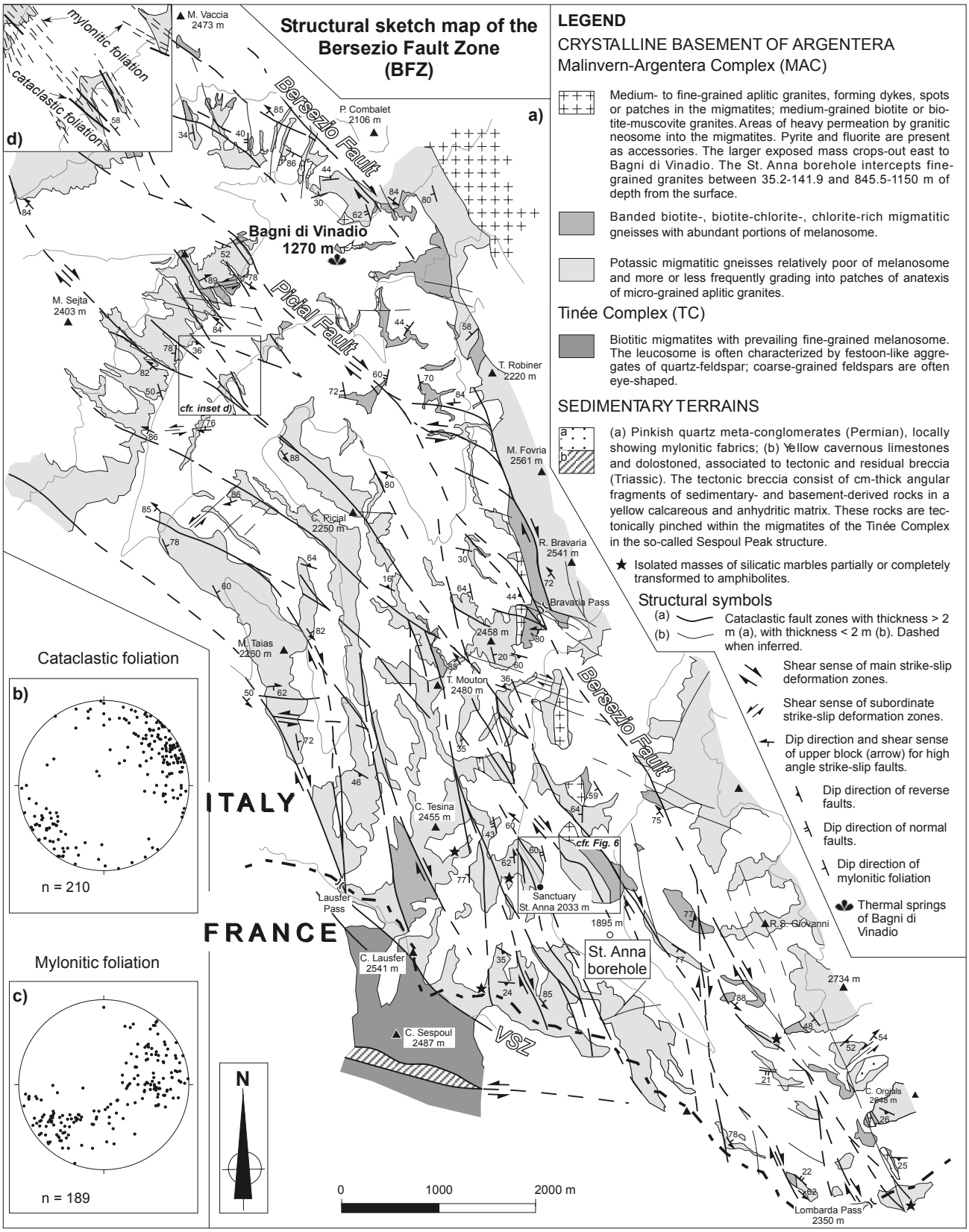

Fig. 4. (a) Structural sketch map of the Bersezio Fault Zone (BFZ). Stereographic plots (equal area projection, lower hemisphere) of (b) cataclastic and (c) mylonitic foliations. The inset (d) provides a scheme of the geometric relationship between the cataclastic and mylonitic foliations.

of tectonic inversion cannot be invoked to justify the discrepant kinematic behaviours.

Interlinked systems of strike-slip and reverse faults occur in the wrench–contraction domains (D1–7). The strike-slip faults occur mainly in two sets: predominant NW–SE right-lateral faults (D1, 2, 3, 6, 7) and subordinate ENE–WSW left-lateral faults (D1–7). Oblique-reverse faults occur in a NW–SE to WNW–ESE system. The distribution of the P-(shortening) and the T-(extension) axes and relative contours (method of Kamb 1959) are shown on the right side of each plot of Fig. 5. The shortening axis is oriented NNE–SSW in domains D1, 3, 4 and 5, and NE–SW in D6–7. The domains showing extensional strain components (D8–9–10) are sited in the core of the BFZ and are bounded by contraction-dominated domains. Within these domains, the dominant structures are sets of E–W, NE–SW and N–S striking normal faults mutually cross-cutting with NW–SE and NE–SW strike-slip faults. Also, these domains are characterized by a strong partitioning among planes accommodating left- and right-lateral strike-slip, and planes accommodating dip-slip and oblique extension. The P-axes are scattered in D8–9 (along a NNE–SSW plane), while they show a near-vertical shortening axis in D10. The domain D11 is the only one displaying structures characterized by a pure wrench kinematics (Fig. 5) with horizontal P-axes orientated NE–SW.

4.1.2. Frictional regime

High-angle strike-slip faults composed of multiple anastomosing layers of cataclasites and gouges, mainly overprinting earlier mylonites, represent the most prominent structures of the BFZ. The cataclastic and the mylonitic foliations commonly lie sub-parallel or at a low angle, testifying the key role played by the ductile fabrics in controlling reactivations in brittle conditions (Fig. 4d). Owing to the high amount of phyllosilicates in the protolith, the cataclasites are mainly foliated and occur in cm- to m-thick layers composed of a dark green matrix and by clasts with a milky white colour. Black cataclasites rich in a graphite-bearing matrix enveloping clasts of quartz and feldspar also occur locally within the crystalline rocks. Microscopic analysis (Baietto 2007) shows that the cataclasites were not only affected by frictional processes, but also that fluid influx promoted the development of phyllonites that accommodated local ductile deformation. Often, the cataclasites consist of cemented clasts containing fragments of cataclasite that were previously cemented. Gouge bands showing pervasive hydrothermal argillification and mesoscopic ductility are commonly interleaved within the cataclasites. Large displacements (>1 km) along faults are suggested by the valuable thickness (up to 5 m) of some gouge layers, by their spatial continuity along strikes and by the finding of large compositional differences that testify the involvement of different protoliths. Fault breccia made up of centimetre-thick clasts and fractured protoliths are widespread and occur in close spatial association along the external borders of the cataclasites and gouges.

The cataclastic-gouge layers occur in two conjugate systems of strike-slip faults: a dominant NW–SE to NNW–SSE set and a minor NE–SW to ENE–WSW set. Within the foliated cataclasites and the gouge layers, typical fabric associations are represented by conjugate R-(Riedel), P- and Y-shears (e.g. *sensu* Hancock 1985) that are visible on a plane view. Fig. 6a provides a scheme of m-thick cataclastic strands located close to the St. Anna Sanctuary. The shear bands composing these faults show geometries that are consistent with right-lateral displacements (Fig. 6b–d), suggesting that the right-stepped bend occurring in the middle of the map can be interpreted as a restraining bend. On a vertical plane normal to the strike of the Y-shears, other phyllosilicate-rich shears, conjugate with those previously described, locally reorient the Y-shears. These planes, labelled here as N-shears, are pervasive and compose duplex arrays with inverse shear sense (Fig. 6e). Overall, the geometry of the shear bands suggests that these faults developed in a context of transpression that involved oblique dextral simple shear and contraction components. The shortening axis presumably lies in a region that is comprised between the N–S, which is the trend of the R-shears and the NE–SW, that corresponds to the apparent direction of displacement of the inverse N-shears. This is consistent with a sub-horizontal contraction axis with a NNE–SSW direction along the straights and a N–S direction along the bend. Geometrical patterns of shear bands indicating a dextral transpressive regime are not limited to the cataclasites in the surroundings of the St. Anna Sanctuary, but were observed locally along almost all the main NW–SE striking faults composing the BFZ. As previously underscored by Perello et al. (2001), the Vinadio thermal springs emerge through a damage zone corresponding to the releasing step-over domain that is bounded by the right-lateral Bersezio Fault and the Picial Fault (Fig. 4a). Poles to main cataclastic foliations cluster in two maxima corresponding to moderately-steeply NE-dipping and SW-dipping planes (Fig. 4b), respectively prevailing in the western and in the eastern sector of the BFZ. These characters are indicative of an overall upward divergent fault geometry (i.e. a flower structure).

4.2. The Terme di Valdieri sector

The structural setting of the Terme di Valdieri sector is similar to the one of Bagni di Vinadio in that it is mainly characterized by the occurrence of several regional strands of strike-slip cataclastic faults oriented NW–SE. Similarly to what is observed at the thermal site of Vinadio, the Valdieri thermal waters discharge from intensely fractured aplitic dykes between the Lorusa Fault and the Cougne Fault (Fig. 7). Geologically, the Terme di Valdieri sector belongs to the Malinvern–Argentera Complex and is mainly composed of igneous rocks and migmatites. The former are constituted by a large body of medium- to coarse-grained granite and by leucocratic aplites and the latter by biotite-rich embrechites and by leucocratic anatexites. The migmatites crop out in the northern part of the mapped sector, while in the southern part the granites are prevalent (Fig. 7a).

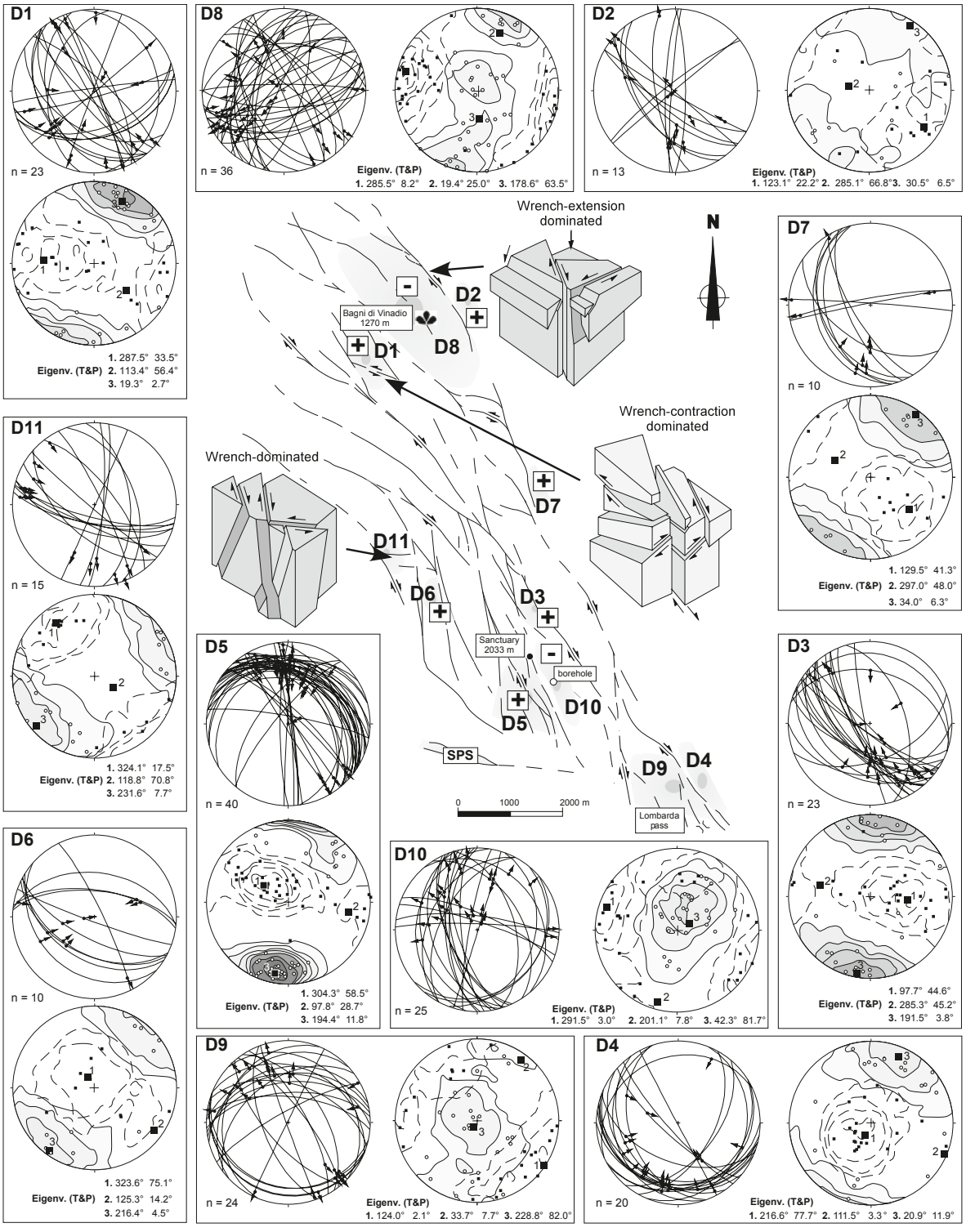

Fig. 5. Sketch map of different deformational domains with Schmidt stereoplots of the slickensides. Each domain is defined on the basis of the local predominance of some types of structures with internally consistent kinematic associations over others. Gradient greys indicate that a precise delimitation is arbitrary anyhow, while black lines correspond to the cataclastic faults shown in Fig. 4. The three block diagrams are a graphical representation (not to scale) of kinematic patterns observed between mutually crosscutting slickensides in different deformational domains. *Fault plane diagram*: great circles display the attitudes of fault planes, with the relative sense of movement of the hanging-wall is indicated by arrows. *P- and T-axes diagram*: P-axes (white circles) and T-axes (black small squares); data are relative to single fault slip data. Grey and dashed contours represent respectively the 2σ standard deviation (contour interval: 2) of Kamb's (1959) contour for the P- and the T-axes. Big black squares represent the global incremental strain axes (1, 2 and 3 indicate the incremental extension, intermediate and shortening axes, respectively).

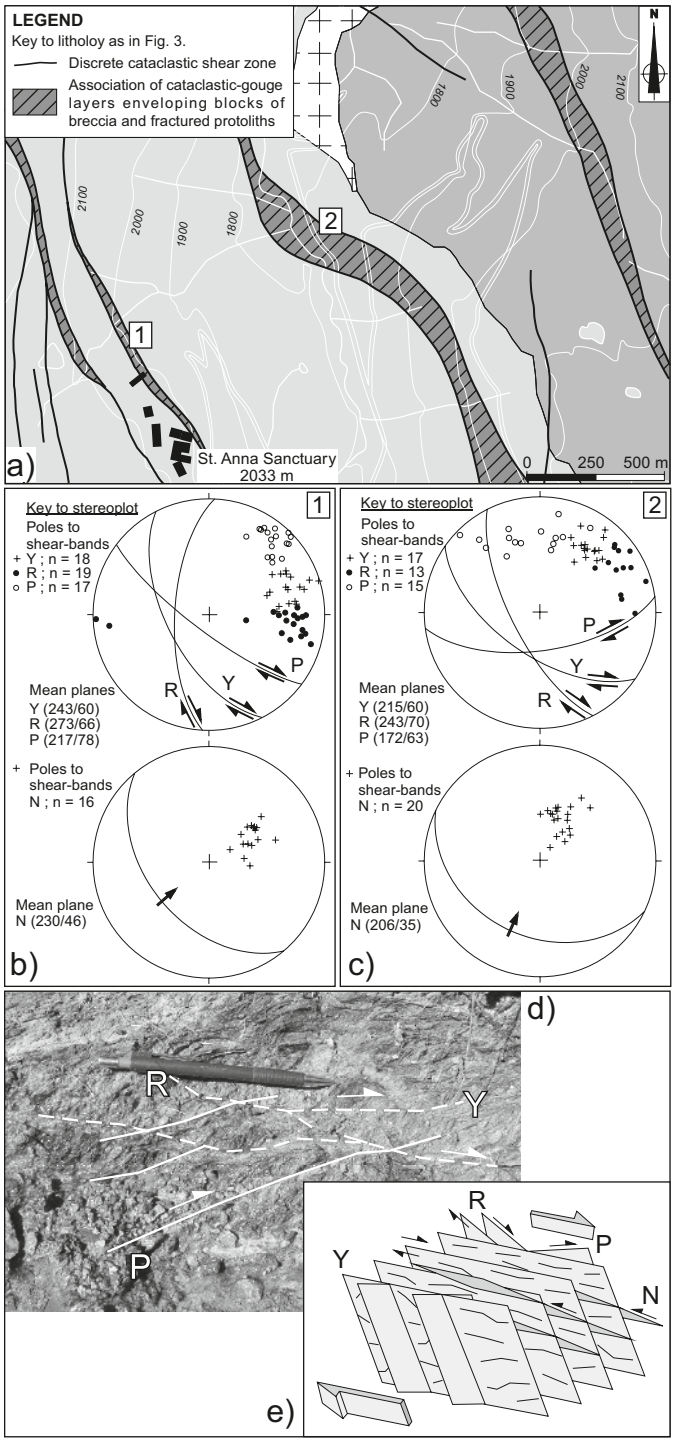

Fig. 6. (a) Sketch map displaying the occurrence of cataclastic-gouge strike-slip faults in the area close to the St. Anna Sanctuary in the core of the BFZ. (b) and (c) are stereoplots (equal area projection, lower hemisphere) relative to the orientation of the main shear bands observed within these faults. (d) picture showing shear bands within cataclastic layers. (e) cartoon depicting the geometric relationship of the shear bands. R-(Riedel), P- and Y-shears (e.g. *sensu* Hancock, 1985) are conjugate shears observed on the map view, while N-shears are here used to indicate shears observed on a normal plane. The angle between the Y- and R-shears is of ~30° in both plots and the average angle between the Y- and P-shears is lower along the straight (26°) than along the bend (43°).

Next to Terme di Valdieri, the migmatites crop out and overlie the granites at shallow depths. In addition, the occurrence at depth of a large granitic body is testified by the Ciriegia Tunnel (located at ca. 1 km from Terme di Valdieri (Bortolami & Grasso 1969), which crosses at some hundreds of metres of depth granites over a distance of two kilometres. Unlike the BFZ, in this region the cataclastic and the mylonitic foliations lie at high angles. This feature is particularly evident in the southern sector of the map in Fig. 7a, where the boundaries of a main E–W striking mylonitic shear zone, namely the Fremamorta Shear Zone (FMS; Fig. 7) occurs. In this sector, NW–SE striking cataclastic faults dissect the FMS at various locations. This belt, which has represented a first-order shear zone in the AM under viscous conditions, is mainly composed of mylonitic and ultramylonitic rocks that crystallized in greenschist metamorphic conditions. The mylonitic foliation dips to the south and to the north at moderate–high angles. A lineation plunge toward the N and the imbrication of mylonitic shear bands indicate that the FMS underwent left-lateral and S-directed inverse displacement.

4.2.1. Frictional-to-viscous regime

Slickensides coated by quartz and chlorite fibres are broadly diffused in the sector around Terme di Valdieri, where they show a persistence ranging from a few metres up to fifty metres. As for the BFZ sector, the kinematic indications that are provided by the fibres grown on the slickensides reveal the occurrence of adjacent structural domains that have been affected by contrasting kinematic behaviours, either with transtensive or transpressive deformation. Figs. 8a–b display the kinematic data of slickensides collected, respectively, in the northern and in the southern mapped sectors of Fig. 7. To the north (Fig. 8a), the slickensides are present mainly in NNW–SSE and ESE–WNW systems, respectively characterized by right- and left-lateral strike-slip components. Dip-slip components, mainly normal, are also present, suggesting that at viscous–frictional conditions, the zone comprised between the Lorusa and Cougne Fault deformed in a wrench, slightly transtensive, tectonic regime. The distribution of the P-axes are consistent with a NNE–SSW direction of shortening. To the south (Fig. 8b), E–W striking faults are dominant over other systems. The kinematic indicators associated with these faults suggest oblique-inverse shear senses. The distribution of the P- and T-axes are consistent with a NNE–SSW oriented shortening and a NW–SE oriented extension.

4.2.2. Frictional regime

The structural setting around Terme di Valdieri is dominated by NW–SE to NNW–SSE directed faults showing discontinuous en-échelon distribution and evidence of right-lateral displacement. These faults cut pervasively through both the migmatites and the granites with a persistence of 1 up to 10 km. Subsidiary ENE–WSW to NE–SW faults characterized by

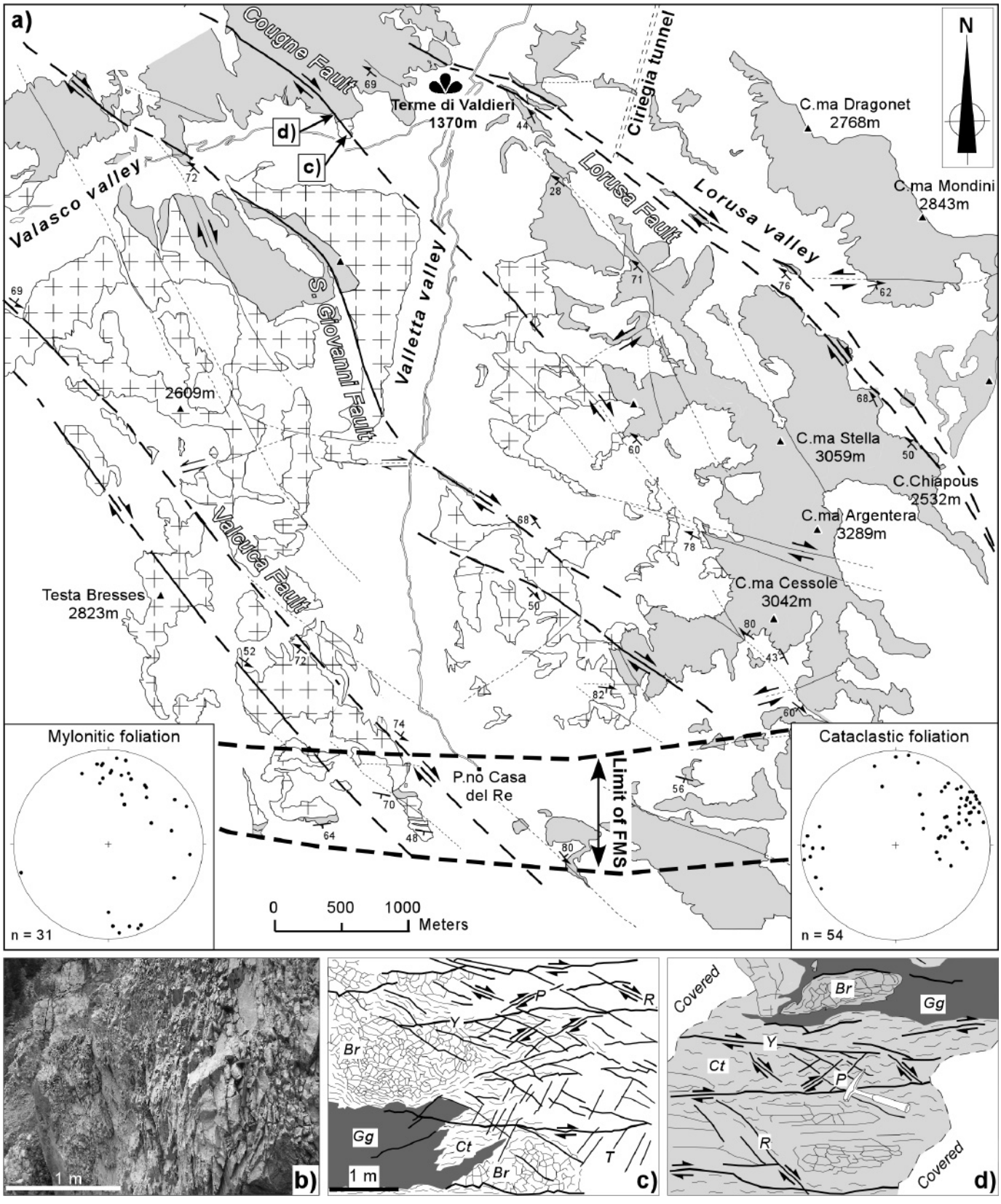

Fig. 7. (a) Structural map of the area surrounding the Terme di Valdieri springs; legend as in Fig. 4, (b) fault breccia with a thickness of several metres developed within the granites, (c) and (d) sketch of the fault rock distribution and shear band relationships along the Cougne Fault in granites and migmatites, respectively.

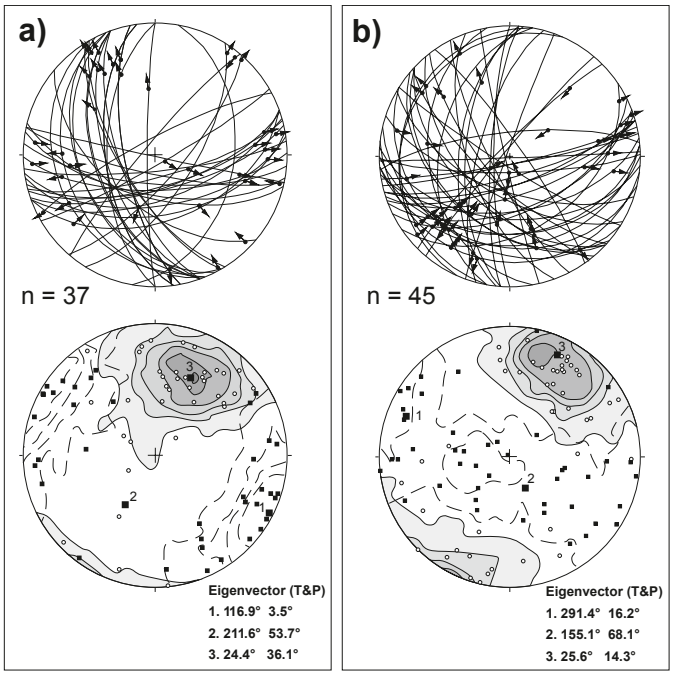

Fig. 8. Schmidt stereoplots with the kinematic criteria associated with the qz–chl slickensides in the northern (a) and southern (b) sector of Fig. 7. Key to symbols in plots as in Fig. 5.

left-lateral movements are associated with the main system. Examples of main faults are the Lorusa, Cougne, S. Giovanni and Valcuca Faults (cfr. Fig. 7a). Similarly to the BFZ, these faults are characterized by associations of cataclasites, gouges and variable amounts of fault breccia and zones of fracture. However, slightly different fault architectures can be observed within the migmatites and the granites. The structure of the strike-slip faults developed within the migmatites is characterized, from the inner to the outer part of the fault zone, by a narrow gouge zone (where most of the slip is accommodated), by an intermediate zone of foliated cataclasites and by an outer domain of tectonic breccias and highly fractured rocks. The gouge, the cataclastic and the breccia zones have thickness ranging, respectively, between 0.1 to 2, 0.5 to 5 and 1 to 50 metres. In contrast, within the granites, the same strike-slip faults are associated with less abundant cataclastic and gouge zones, and show comparatively wider zones (hundreds of metres thick) where the breccia and the intense fracturing are prevalent (Fig. 7b). As a result, these zones of intense fracturing are widespread and not only limited to the borders of the main faults. In these domains, the fracture spacing ranges from a few centimetres to a metre, while the opening is usually of a few millimetres.

The Cougne Fault crosscuts either the migmatites and the granites generating in both lithologies heterogeneous associations of different fault rocks and complex through-going geometries. The geometry of the cataclastic shear bands, composed of Y-shears, R-shears and P-shears, allows the recognition of right-lateral shear senses. The Y- and R-shears appear to be the most penetrative fabrics (Figs. 7c–d). Other scarcely penetrative shear bands, named X-shears (*sensu* Hancock 1985), located at a high-angle with respect to the Y-shears, offset all the other shear bands. Presumably, the T-shears developed during progressive deformation as a result of a lock-up of the other shears.

The Valdieri thermal springs discharge along the western edge of the right (contractional) step-over region between the Lorusa Fault and Cougne Fault, in a zone of intense fracturing. The Lorusa and Cougne faults dip south-westward while, moving to the south, the S. Giovanni and the Valcuca faults show a progressive north-eastward rotation of the dip direction that defines a regional scale flower structure, similarly to the BFZ geometry observed around Vinadio.

4.3. The Berthemont-Les-Bains sector

The thermal springs of Berthemont-Les-Bains up-well on the south-western border of the AM, close to the contact with the Dauphiné–Helvetic covers. The springs consist of four groups of waters discharging within the migmatites at different locations and elevations (Fig. 9). The main springs are the so-called Saint-Jean Baptiste (SJB) and Saint Julien (SJ), which are sited close to the intersection of the faults of Lancioures, Férisson and Louchio. The two other springs, namely Saint Michel (SM) and Campas, discharge along the cataclastic fault of Lancioures, at higher altitudes with respect to SJB. The Lancioures and Férisson faults show evidence of right- and left-lateral displacement, respectively. All the waters discharge along narrow single fractures located at the margins of the Lancioures Fault in undeformed portions of the migmatites. Besides, the damage zone of this fault is much thinner and less strained compared with the ones found at Vinadio and Valdieri. In the Berthemont sector, the only type of structures occurring are those that can be attributed to frictional–viscous and frictional conditions of deformation, while mylonitic rocks typical of a viscous deformation regime are not present. In the mapped area, the basement rocks are characterized by migmatitic gneisses with a mean foliation dipping moderately to the NW. In the mapped area, the massif boundary is marked by Permian siltites lying unconformably on the crystalline rocks and by tectonic surfaces separating the post-Permian rocks from the migmatites. Post-Permian rocks are represented by Triassic cavernous limestones and dolomites, mostly associated with yellow cargneules and Jurassic limestones and dolostones. All the cargneules found in this area are pervasively tectonized and show evidence of fluid leaching processes.

4.3.1. Frictional-to-viscous regime

Similarly to the other examined Argentera thermal sites, frictional–viscous-related structures, such as quartz–chlorite striated slickensides, are widespread around Berthemont. In this region, several S-C shear bands displaying ductile–brittle char-

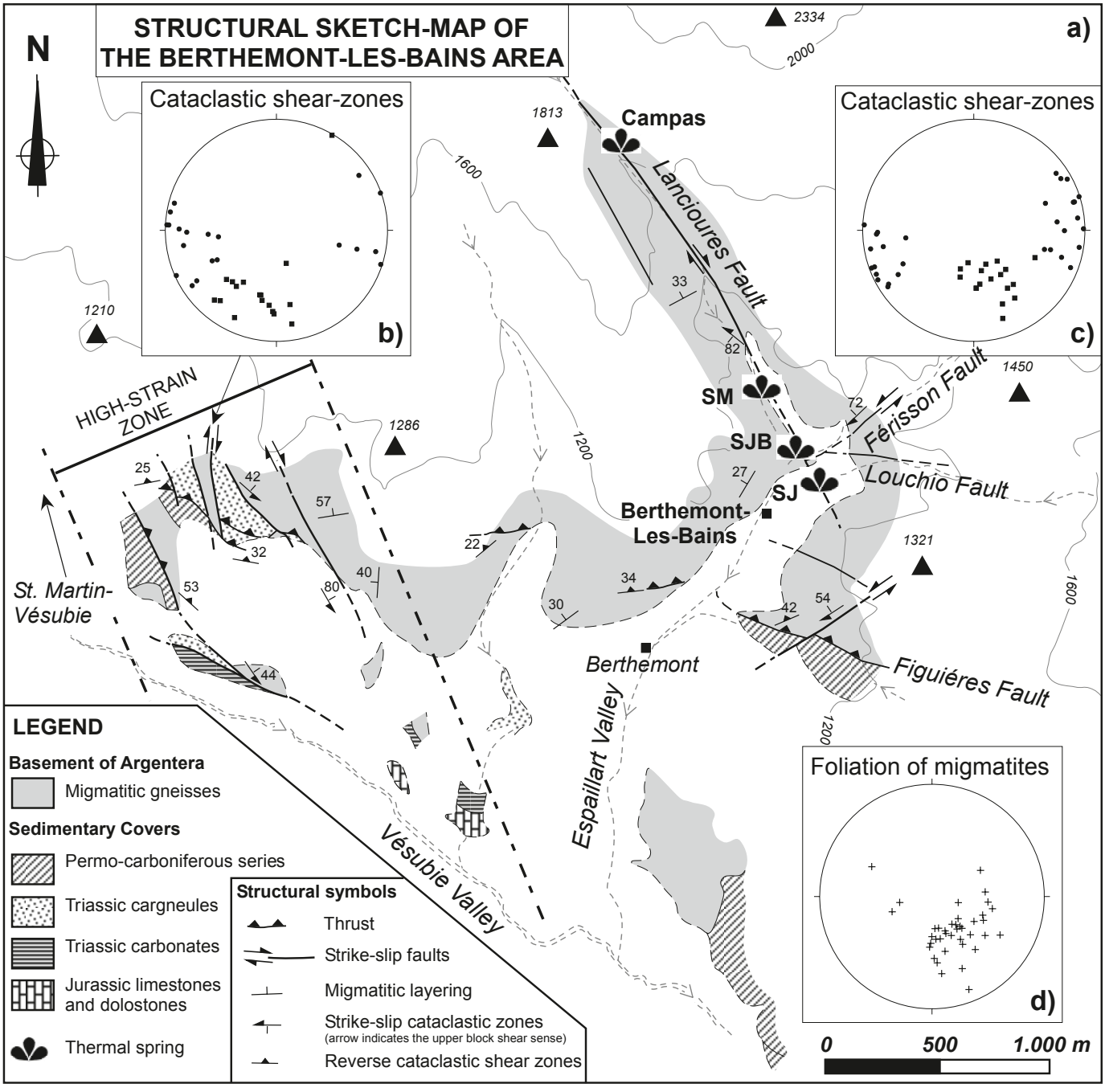

Fig. 9. (a) Structural sketch-map of the Berthemont-Les-Bains sector; SM: Saint Michel spring, SJB: Saint Jean-Baptiste spring, SJ: Saint Julien spring. Stereoplots (equal area projection, lower hemisphere) with poles to cataclastic shear zones in (b) a high-strain domain where the migmatitic gneisses are found repeatedly in tectonic contact with the Dauphiné–Helvetic sedimentary covers and (c) in a less deformed domain located more internally within the migmatitic gneisses. (d) Schmidt stereoplots with poles to migmatitic foliation.

acters were also observed and attributed to the same deformational regime. All these features occur mainly within the migmatites and the Permian siltites. Overall, the qz–chl slickensides accommodate dip-slip and minor oblique-slip components (i.e. pure strike-slip is not observed), and the fibres' steps indicate ubiquitous normal displacement. In the eastern sector, the normal and oblique–normal faults are E–W to ENE–WSW oriented (Fig. 10a), whereas, in the western sector, they are partitioned on multiple sets NE–SW, E–W and NW–SE striking (Fig. 10b). The NW–SE faults crosscut through the migmatites and the Permian schists, allowing a normal offset toward the NE of the covers with respect to the basement. The scatter plot

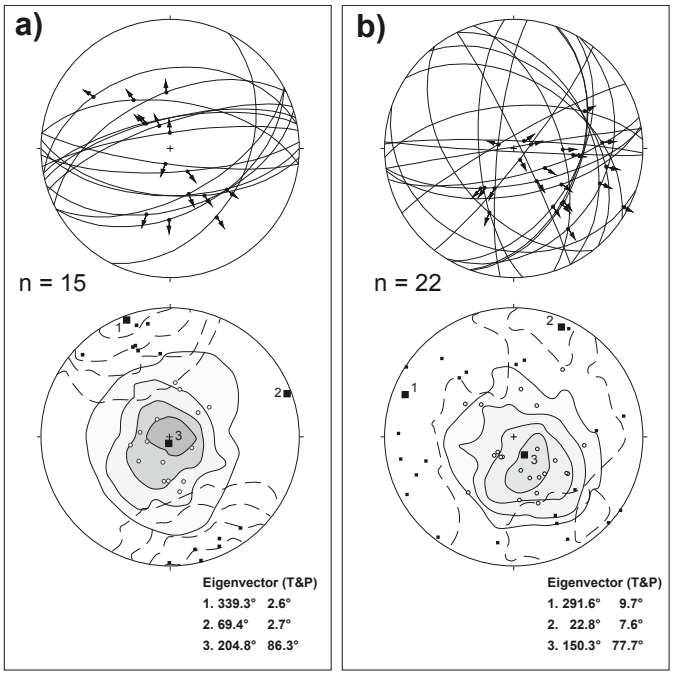

Fig. 10. Stereoplots (equal area projection, lower hemisphere) with the kinematic criteria associated with the qz–chl slickensides in the western (a) and eastern (b) sectors of Fig. 9. Key to symbols in plots as in Fig. 5.

and contours of the P- and T-axes relative to the slickensides indicate a sub-vertical shortening axis and a sub-horizontal extensional WNW–ESE to NNW–SSE oriented axis (Figs. 10a–b). Shear bands of type S-C with ductile–brittle characters are widespread in the western sector of Fig. 9, while in the eastern sector they have not been observed. In the migmatites, these fabrics consist of a protomylonitic foliation (S-shears) and a locally penetrative foliation defined by mm-thick aligned chlorite foliae (C-shears). In the Permian siltites, these fabrics are marked by penetrative cleavages with a mm spacing. The C-shears strike NW–SE, dip gently toward NE, and the deflection of the S-shears indicates normal displacements along these planes, suggesting that these features developed in a tectonic context that is similar to the one of the qz–chl slickensides.

4.3.2. Frictional regime

Systems of cataclastic strike-slip faults and reverse faults crosscut all the lithologies shown in the mapped sector (Fig. 9a) and the previously described structures. These features can be observed in the whole mapped area, even though the western sector represents a high-strain zone that has undergone higher degrees of strain than the eastern sector. The strike-slip systems are constituted by main NW–SE to NNW–SSE and by E–W to NE–SW striking faults, respectively characterized by right-lateral and left-lateral displacements (Figs. 9a–b). These faults are linked to systems of E–W reverse faults that show an apparent top-to-the-S sense of displacement. However, these structures are scarcely persistent and are subordinate with respect to the systems of strike-slip faults. Their geometry suggest that the reverse faults acted as contractional steps connecting the high-angle NW–SE striking faults.

The highly deformed western sector of the map of Fig. 9a is crosscut by very closely spaced, anastomosing and coalescing cataclastic-gouge layers. These layers bound blocks of fractured migmatites and breccia with sizes ranging from a few cm to several m. These faults also constitute tectonic contacts repeatedly separating the crystalline rocks from the covers. The tectonic contact between the migmatites and the sediments occurs through disrupted sequences of Triassic cargneules made up of cm-thick fragments of limestones embedded in a matrix of yellow residual breccia. In the eastern sector of the map, where the springs of Berthemont are located, the cataclastic faults are ~1 m thick and are characterized by much wider spacing than the faults observed in the western zone. The damage zones are developed along the borders of the faults and have thickness of a few decimetres up to a metre, while the fault core is usually very thin. The most persistent structure identified on the field is the NW–SE striking Lancioures Fault. Other structures are the NE–SW striking Férisson Fault and the E–W striking Louchio Fault. The Figuiéres Fault, which Romain (1985) already recognized as a top-to-the-S reverse structure separating the basement from above the covers, is structurally linked with a NE–SW striking high-angle fault that represents a left-lateral ramp (Fig. 9c). The kinematic indicators observed in both the western and eastern zones are consistent with the occurrence of a transpressive regime accommodated both by wrench and reverse shear components. The axes of shortening of these structures are broadly NNW–SSE oriented. In summary, this observation contrasts with the kinematic information obtained for the structures attributed to the frictional–viscous regime.

4.4. Hydraulic and thermal characters related to the AM fault zones

The structures that formed in a viscous and in a frictional-to-viscous regime represent fossil conduits that focussed various thermal fluid flows. Subsequently, the original permeable networks were, in part, affected by mineral deposition that provoked the sealing of the circulation systems. Besides, the fault zones that developed in the frictional regime reactivated part of the old shears, promoting active fracturing and enhanced fluid flow despite clogging by hydrothermal mineral precipitates. In general, these fault zones constitute the main pathways for the present thermal circulations. A major evidence of the hydraulic control imposed by these structures is provided by the spatial relationships between the thermal springs and the cataclastic fault zones. At Vinadio, as already documented by Perello et al. (2001), the springs are located in a zone of extensional step-over linking two NW–SE striking right-lateral faults (Fig. 11a). Conversely, at Valdieri, the springs are located in a zone of enhanced fracturing, corresponding to a contractional step-over within other NW–SE striking faults (Fig. 11b).

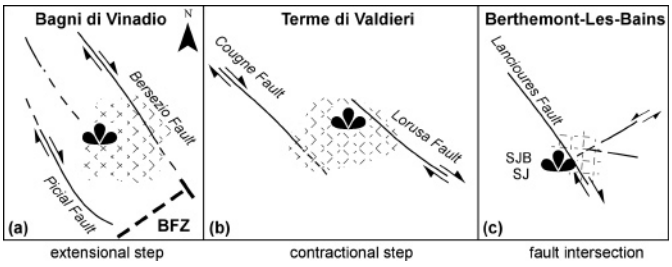

Fig. 11. Schematic diagrams showing "breakdown" regions (i.e. zones of enhanced fracturing) in zones of fault interaction and fault intersection. (a) Setting of Bagni di Vinadio with the thermal springs located within an extensional step along the BFZ. (b) Setting of Terme di Valdieri with the thermal springs located next to the Lorusa Fault. In this region, the enhanced fracturing can be imputed to the contractional step along between the Lorusa and Cougne faults. (c) Setting of Berthemont-Les-Bains with the SJB (Saint Jean-Baptiste) and SJ (Saint Julien) springs located in a zone of fault intersection.

At Berthemont, the thermal springs occur close to the fault intersection (Fig. 11c).

A general description of the hydraulic behaviour of these fault zones is proposed following the criteria adopted by Caine et al. (1996). At Berthemont, the fault zones display a relatively high proportion of high-permeability elements (i.e. breccia and fracture zones), while low-permeability elements (i.e. cataclastic and gouge layers) are only locally present, implying that these faults act principally as conduits for fluid flow. Besides, in the Vinadio and Valdieri sectors, the faults display multiple cataclastic-gouge strands that envelope lens-shaped blocks of breccia and fractured rocks. These fault zones may contemporaneously act as impermeable barriers to cross-fault flow and as conduits for along-fault flow, on the whole contributing to the formation of metre- to hundreds-of-metres-scale complex systems of conduits and barriers. Qualitatively, it can be supposed that in these fault zones the main and the minor axes of the permeability tensor are oriented, respectively, parallel and perpendicular to the strike of the cataclastic zones. However, the inherent complexity of these systems emphasizes the difficulty of obtaining a deterministic assessment of the permeability tensor distribution. In the Bersezio Fault Zone, slug tests carried out in the St. Anna borehole (Darcy 1997) point out damage zone permeabilities higher than 1×10^{-14} m^2, and a permeability contrast of over 400 times between the damage and the core zones (Baietto 2007). However, the rheological behaviour of lithology also plays a key role in controlling the fault zone hydraulic architecture within the AM. While migmatitic gneisses mainly deform by cataclasis and fractures are accommodated on the borders of main fault zones, granites deform mainly by fracturing such that moderate- to high-fracture density regions are distributed over wider rock volumes that are not exclusively limited to the borders of fault zones. By studying the core data of the St. Anna borehole, Baietto (2007) estimated that 90% of the granites against 20% of the migmatites (relative to the total rock volumes that were affected by frictional deformation) underwent fracturing. The state of fracturing of the granites that involves large rock volumes, as opposed to the fracturing within the migmatitic gneisses that is mostly concentrated along localized damage zones, creates the conditions for pervasive diffuse flows in the granites and focussed flows in the migmatitic gneisses.

Groundwater flowing through the main fault systems produces drastic thermal perturbation within the massif. These perturbations can be evaluated by considering the different temperatures: at Bagni di Vinadio thermal waters up-well with temperatures up to 65 °C, while in the St. Anna Valley (ca. 6.5 km southward of the Bagni di Vinadio springs), the St. Anna borehole shows that waters flowing within the BFZ have a temperature of only 24 °C at depths of 1150 m (Darcy 1997). As the surface mean annual temperature is 8 °C, the resulting local geothermal gradient in the borehole appears to be as low as ca. 14 °C/km. Similarly, the occurrence of a negative thermal anomaly induced by the infiltration of cold shallow waters through a fault zone is evidenced by the temperature profile within the Ciriegia Tunnel, in the Valdieri sector (Fig. 7). At the interception of this tunnel with the Lorusa Fault (about 1 km east of the Valdieri thermal springs and ca. 600 m below the surface), the reported inflows were of 20 l/s with temperatures of 20 °C, indicative of an apparent geothermal gradient of ca. 19 °C/km (Bortolami & Grasso 1969). Also at Berthemont, boreholes as deep as 450 m and located a few metres away from the main thermal springs reported temperatures at depth that are lower than those of the springs, indicating adjacent zones of negative and positive anomaly. The location of the positive and negative thermal anomalies and the spatial distribution of the more permeable fault components allow us to define a scheme for the recharge of superficial waters. Fig. 12 provides a delimitation of the catchment areas where the cold meteoric waters are inferred to infiltrate toward the deep thermal reservoirs that feed the thermal springs of Vinadio, Valdieri and Berthemont.

5. Discussion

5.1. Late-Alpine structural evolution of the thermal spring areas

The structural analysis of the Bagni di Vinadio, Terme di Valdieri and Berthemont-Les-Bains sectors has revealed that the Argentera Massif experienced protracted late-Alpine deformation under viscous, frictional-to-viscous and frictional conditions (*sensu* Schmid & Handy 1991). These deformations accompanied the progressive exhumation of the AM and brought about the development of complex assemblages of structures and fault rocks whose hydraulic properties have been playing a key role in channelling the past and present thermal flows. This study highlights that deformation occurring at different crustal levels yielded different types of strain localization, which in turn influenced different patterns of flow of thermal fluids. A major shortcoming is that direct dating of faults that formed starting from frictional-to-viscous is lacking for the entire southern part

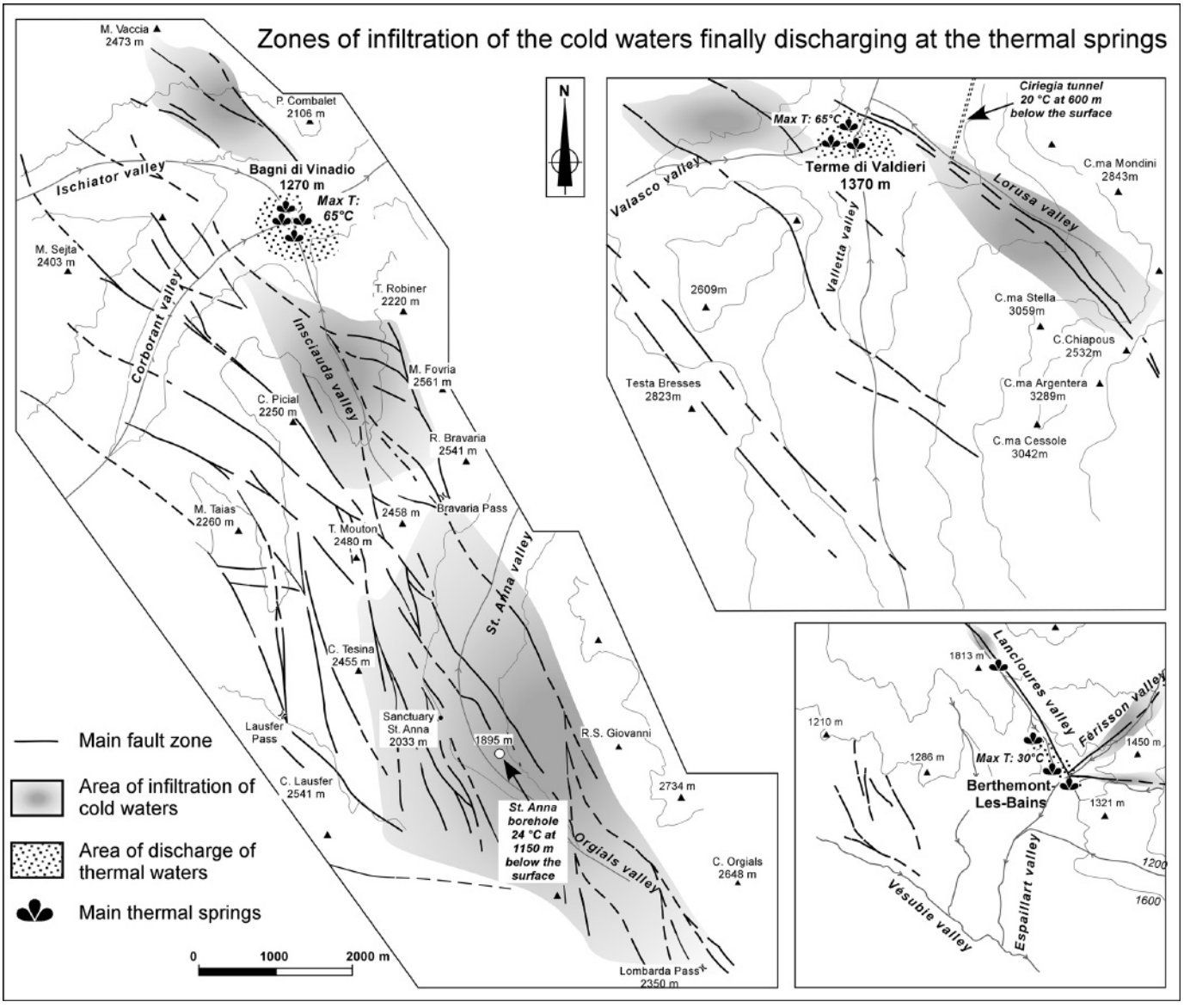

Fig. 12. Sketch of the inferred recharge zones where the meteoric waters infiltrate at depth, feeding the geothermal reservoirs and sustaining the discharges at Bagni di Vinadio (a), Terme di Valdieri (b) and Berthemont-Les-Bains (c).

of the Western Alps. The only relative constraints are provided by the fission track ages of blocks bounding faults (Bogdanoff et al. 2000; Bigot-Cormier et al. 2000).

Deformation under viscous conditions brought about the development of thick mylonitic belts cross-cutting the entire AM. In particular, the Bersezio Fault Zone (BFZ) and the Fremamorta Shear Zone (FMS) represent first-order structures that controlled the tectonic evolution and the pathways of regional fluid flows at this stage (Fig. 13). Within the BFZ, the mylonitic shears developed in NW–SE to N–E striking strands under right-lateral transcurrent shear, while the FMS mylonitic belt formed under E–W striking left-lateral and reverse shear in a transpressive context. In the studied FMS sector, the reverse shears occur along mylonitic planes both S- and N-dipping, while according to Malaroda et al. (1970), the mylonites on the eastern prosecution of the FMS accommodated top-to-the-S reverse displacement on planes gently dipping to the north (Fig. 13). Summing up, it is likely that the BFZ behaved as a right-lateral ramp linked with the southward thrusting along the FMS of the north-eastern part of the Argentera above the rest of the massif. This scenario was already proposed by Tricart (2004), who ascribed this event to the Pliocene. However, according to the dating studies recently carried out by Corsini et al. (2004) on the synkinematic phengites (i.e. 22.5 Ma) grown within the mylonites, we propose that this tectonic event was active during the Early Miocene. Also, the age of 22 Ma that

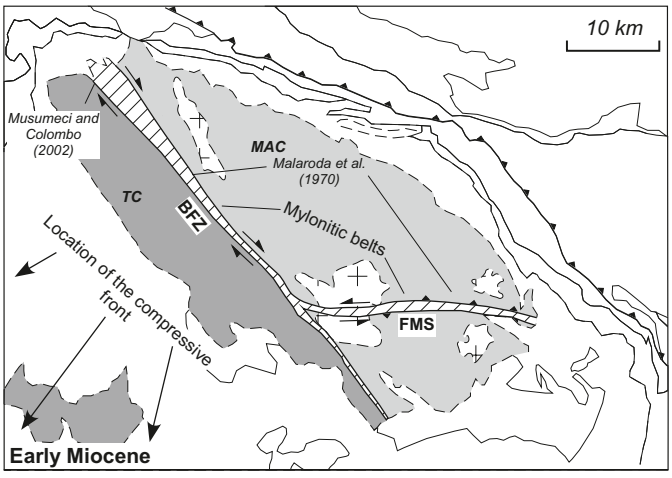

Fig. 13. Sketch of the tectonic setting of the Argentera Massif during the Early Miocene. During this period, the AM was experiencing transpressive deformation at viscous conditions that brought about the development of regional mylonitic belts, namely the BFZ and the FMS. The dashed line around the AM indicates that the massif was deeply buried at this time. The black frames display the areas investigated in the present work. For the location of the internal and external compressive fronts cfr. Campredon & Giannerini (1982), Labaume et al. (1989), Guardia et al. (1996) and Laurent et al. (2000).

was constrained by zircon FT data by Bigot-Cormier et al. (2000) for the strong pulse in the cooling rate that accompanied the early AM uplift seems consistent with this interpretation. Speculatively, this event was related to the southward thrusting of the Helminthoid Flysch that is also believed to have taken place during the Early Miocene (Campredon & Giannerini 1982; Labaume et al. 1989; Guardia et al. 1996; Laurent et al. 2000).

Deformation at frictional–viscous transition affected diffusely all the examined sectors of the massif and resulted in the development of slickensides coated by fibres of quartz and chlorite. The kinematic indicators associated with these structures suggest that the central and the western sector of the massif experienced different tectonic conditions (Fig. 14a). Within the central BFZ, the strain partitioning yielded complex kinematic patterns with domains separated by NW–SE faults. Each domain is individually characterized by combinations of predominant wrench–contraction and minor wrench–extension components. These features provoked, respectively, the development of local push-ups and pull-aparts. Within the FMS and in the adjoining internal sectors, the slickensides exhibit kinematic characters consistent with a bulk transpressive regime, despite local transtensive structural associations also being present. Since evidence of tectonic inversion was not observed in these areas, it is proposed that these structures with contrasting kinematics can have formed coevally in a context where transpression dominated (Fig. 14b), while transtension arises locally as the product of structural anisotropies (e.g. mylonitic foliations) and complex strain partitioning. This behaviour is particularly evident in the BFZ where the contractional domains bound externally the extensional ones (cfr. Fig. 6), indicating that transpression acted as a regional boundary condition. It has been documented that this kind of kinematic feature represents a common occurrence in transpressive settings that undergo complex strain partitioning (Dewey et al. 1998). Overall, the BFZ and FMS sectors show shortening axes (excluding the transtensive domains) which are consistent with a sub-horizontal NNE to NE direction.

Around Berthemont, kinematic indicators such as normal E–W and NW–SE slickensides associated with extensional S-C shears testify that an extensive rather than a transpressive

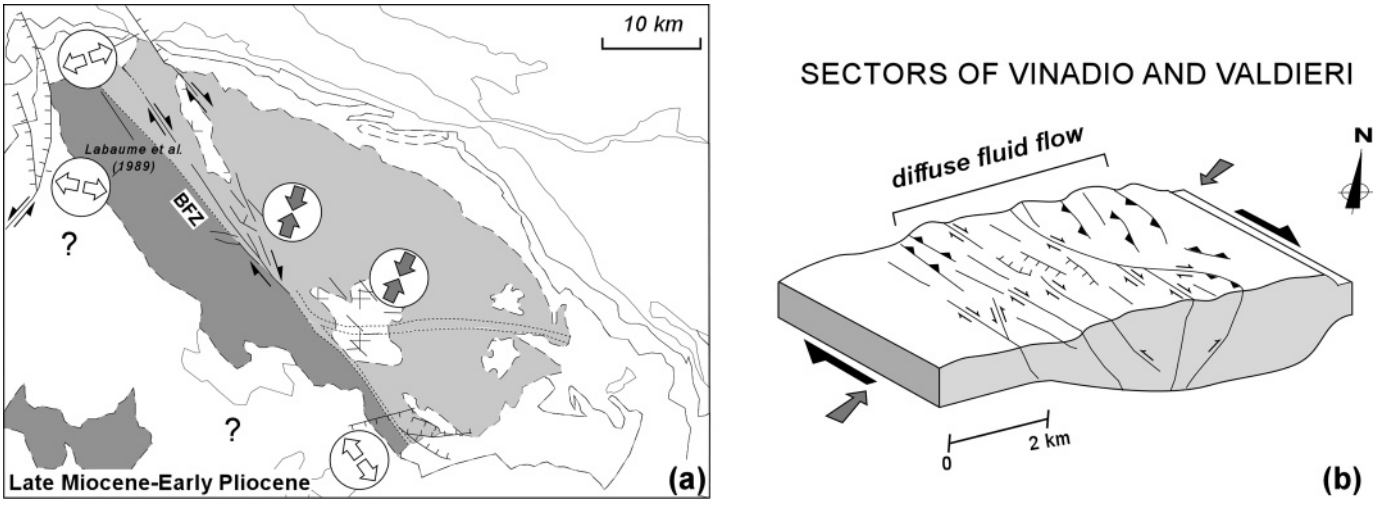

Fig. 14. (a) Sketch of the tectonic setting of the Argentera Massif during the Late Miocene–Early Pliocene. During this period, the massif was experiencing diffuse deformation under a frictional-to-viscous transition resulting in the development of low-strain structures. The central part of the massif recorded a bulk transpressive regime while the north-west and the south-west extremities of the massif underwent extensional conditions. (b) Block diagram displaying the tectonic and hydraulic setting of the Vinadio and Valdieri sectors during this deformation stage.

regime affected the western border of the massif under frictional–viscous conditions. On the north-western extremity of the AM, Labaume et al. (1989) documented the existence of sets of NNW–SSE normal faults, suggesting that an extensional regime might have affected the entire AM external margin. These authors also observed that during this stage the northern branch of the BFZ behaved as a normal fault that accommodated down-to-the-NE displacement. In addition, other systems of normal faults have been reported for the Briançonnais–Queyras area between the Pelvoux and Argentera transect. In this sector, Sue & Tricart (2003) and Tricart et al. (2006) describe the existence of normal faults characterized by a multitrend extension, which were subsequently reactivated in a transcurrent regime. While it is apparent that, from the northern to the southern border of the AM, the direction of extension varies by several degrees, other structural data suggest that, in the northernmost part of the Western Alps, an extensional phase took place with a predominant orogen-parallel direction of extension (Hubbart & Mancktelow 1992; Steck & Hunziker 1994). According to Sue et al. (2007), the orogen-parallel extension could have been triggered by the existence of a southern free boundary that corresponds to the opening of the Ligurian Sea. This extension is interpreted by these authors as a lateral extrusion of the internal zones to the south, where the Ligurian Sea was opening along the western side of the Adriatic promontory. This tectonic phase, active starting from the Early to Middle Miocene, was coeval with the westward propagation of the compressive front in the external zones. In the AM, there are no elements for supposing that in the frictional–viscous regime the transpressive deformation was coeval with the extensional one. Moreover, while on the northern part of the Western Alps extension dominates in the more internal zones with respect to compression, in the AM this looks to be the opposite. Despite a geodynamic interpretation being beyond the scope of this paper, it is possible that the extensional phase observed in the Argentera Massif could correspond with the orogen-parallel extension documented on the northern side of the Western Alps. However, this hypothesis must be constrained by further structural data because, while the NW–SE direction of extension (i.e. locally orogen-parallel) observed at Berthemont seems consistent with a lateral extrusion model, the other directions of extension documented on the northern border of the massif hardly fit with this scenario. It cannot be excluded that these structures formed more recently instead, during a post-collisional regime where orogen-perpendicular extension affected diffusely the axial part of the Western Alps (Sue et al. 2007). As an hypothesis, extension on the AM external margin could have started taking place coevally with crustal thickening on the internal parts. This could have occurred in a period comprised between 8 and 4 Ma, during which the AM was experiencing a moderate exhumation rate (Bigot-Cormier et al. 2000).

Late deformation in frictional conditions brought about the development of regional systems of faults made up of anastomosing cataclastic-gouge strands enveloping blocks of breccia and fractured protoliths. These faults progressively grew during the final exhumation of the AM that should have taken place from 3.5 Ma with rates of 1.1–1.4 mm/yr, according to Bigot-Cormier et al. (2000). Unlike the frictional–viscous deformation, during this phase, the central and western parts of the massif recorded a similar tectonic history. In the central part of the massif, the cataclastic faults developed in two high-angle strike-slip systems: a dominant set of NW–SE to NNW–SSE faults and a subordinate set of NE–SW to ENE–WSW faults. Several NW–SE faults occur within the BFZ and in the sector hosting the FMS. However, while within the BFZ this system overprints at a very low angle early mylonitic shears (Fig. 15a), in the FMS it crosscuts at a high angle the E–W mylonites. This attests that, while from viscous to frictional deformation the main shearing axis in the BFZ maintained a NW–SE orientation, in the FMS sector it switches progressively from an E–W (left-lateral shear) to a NW–SE (right-lateral shear) orientation. Around Vinadio and Valdieri, the NW–SE faults are arranged in arrays of upward divergent geometries that show both right-lateral and reverse shear components (Fig. 15b). This means that the two sectors are located in zones of a positive flower structure that formed during the final AM exhumation through transpressive wrench faulting (Fig. 15c). It should be noted that Fry (1989) already proposed that, in the frame of the External Arc of Western Alps, the AM could be viewed as a pop-up structure (i.e. a domal uplift with a positive structure that formed in a large intraplate strike-slip system; cfr. Stone 1995). In the Vinadio and Valdieri sectors, the axes of shortening kept a sub-horizontal NNE direction. In the Berthemont sector, the earlier extensional phase recorded at the frictional–viscous transition was followed, under frictional conditions, by a transpressive phase through the development of NW–SE and NE–SW strike-slip faults (Fig. 15a). Also, in the north-western sector, Labaume et al. (1989) documented the occurrence of a compressive phase (N–S shortening) that caused the reactivation of earlier NNW–SSE normal faults as dextral strike-slip faults.

5.2. Patterns of active thermal circulations

The patterns of active thermal circulations of the Argentera Massif are primarily controlled by the structural and hydraulic setting of the fault zones that formed under frictional conditions.

Prior to this phase, different deformational styles brought about different flow patterns. As an example, during the viscous deformation, the BFZ and FMS constituted the main pathways for fluid flow that promoted pervasive mineral reactions in lower greenschist conditions. It is likely that these circulations have also brought about the deposition of sulphides within the BFZ. Fluid inclusion analyses carried out by Facello (2006) on sphalerite minerals recrystallized in mylonitic bands indicate temperatures in the range of 320–380 °C, which is consistent with the temperature (350 °C) constrained by Corsini et al. (2004) for the Early Miocene mylonites. During the frictional-to-viscous deformation, both the internal and the external parts of the AM were affected by a diffuse, even though not penetrative, fluid flow through the massif (Fig. 14b), as testified by

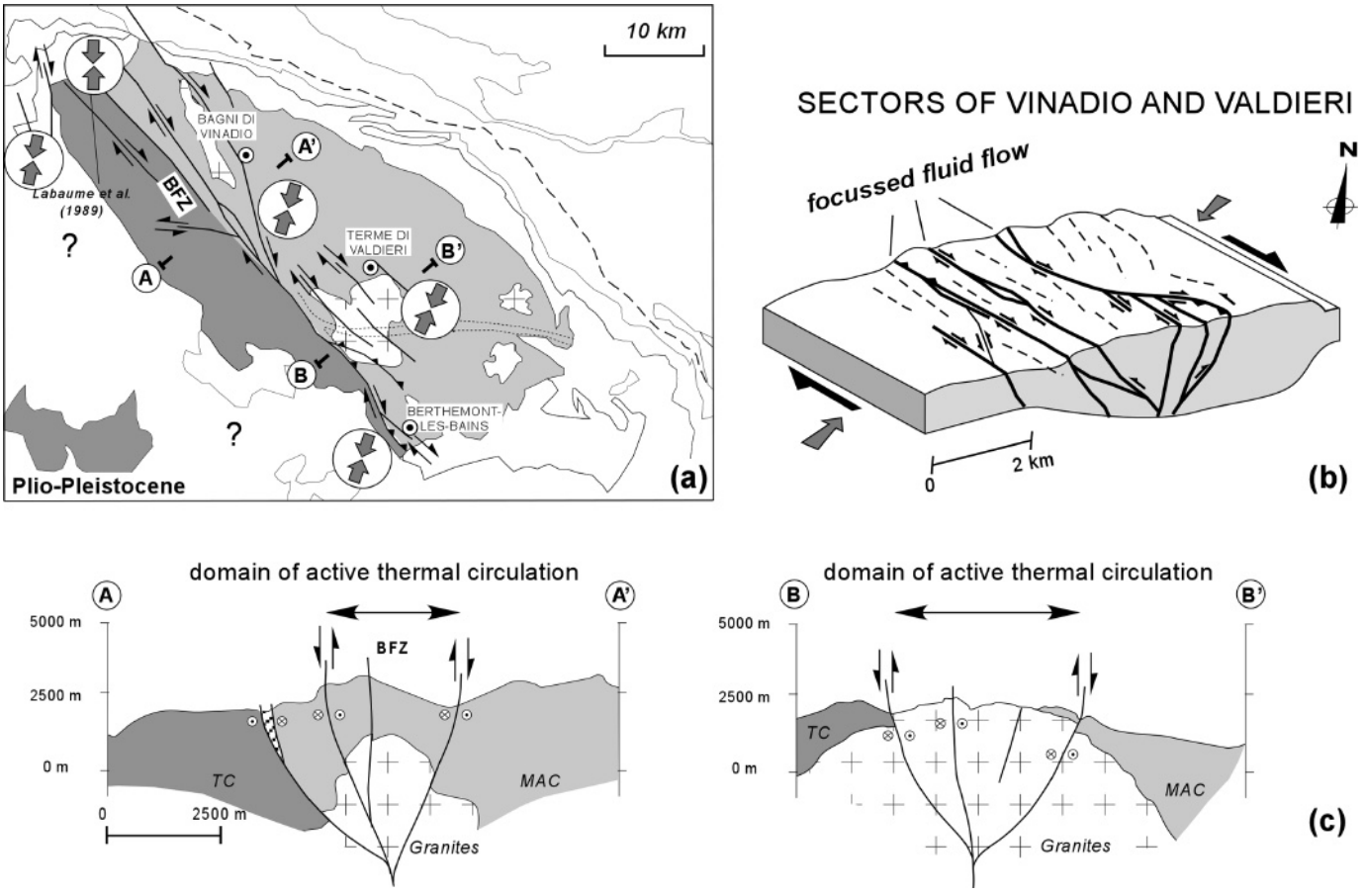

Fig. 15. (a) Sketch of the tectonic setting of the Argentera Massif during the Plio-Pleistocene. Cataclastic fault zones develop at regional scale under a regime of bulk transpression and mainly along systems of right-lateral NW-trending faults. (b) Block diagram depicting the tectonic and hydraulic setting of the Vinadio and Valdieri sectors during this deformation stage. (c) Cross-sections of the Vinadio and Valdieri sectors showing that, at this stage, these areas behave as regional push-up structures accommodating near vertical offsets between adjacent domains. The profiles also display the inferred boundaries for the present-day thermal circulations.

the widespread occurrence of lower-greenschist facies minerals coating the slickensides and filling the veins. With the final exhumation of the massif, the creation of fine-grained fault materials such as cataclasite and gouge has increasingly led to fault weakening and strain concentration. As a result, the high permeable zones have progressively been concentrated along the borders of the main strike-slip faults, resulting in focussed fluid flows such as depicted in the scheme of Fig. 15b. However, the micro-structural evidence of the cataclastic rocks suggests that the fluid flow through these faults has been cyclical and interleaved with multiple episodes of cementation and cataclasis.

Significantly, the thermal systems Vinadio and Valdieri, which are those characterized by the most elevated discharge temperatures of the massif, are both found in step-over zones of extensional and contractional types, respectively (Fig. 11a–b). It is well documented that fault interaction zones occurring in several tectonic settings often host thermal discharges or ore deposits related to hydrothermal activity (Sibson 1987; Curewitz & Karson 1997). Usually, these zones correspond to breakdown regions where stress concentration promotes active fracturing that increases permeability and fluid flow (Segall & Pollard 1980; Scholz & Anders 1994). In the Berthemont sector, fault intersection rather than interaction influences the local enhanced fracturing and the up-well of thermal waters (Fig. 11c). These waters discharge from single sets of fractures instead of being located within a large damage zone as for the two other cases.

At Vinadio and Valdieri, metre- to hundreds-of-metres-scale complex systems of conduits and barriers cause inhomogeneous fluid flow patterns along the fault zones. According to the location within the fault zone, the numerous fractured domains that occur within strands of low permeable material can store fluids or let fluids circulate along the faults. This hydraulic architecture, which is strikingly similar to the one described by Faulkner et al. (2003) in the ca. 1 km-thick Carboneras Fault Zone (South-Eastern Spain), implies the realization of a number of fluid flow and fluid sealing possibilities. Indirect evidence of the occurrence of a fault hydraulic architecture made up of systems of compartmentalized conduits is provided by the observation of the geochemical and physical parameters

of the waters discharging at Vinadio and Valdieri. Despite the close proximity of the spring outlets in the two sites (tens of metres), a range of concentrations of the chemical species and of temperatures suggests that a limited amount of mixing of waters occurs in the fracture networks feeding the springs. This phenomenon is illustrated by the correlation plot between the conservative constituents Cl^-, B and Li^+ and by the spread of point observed in the Na^+ vs. Cl^- and $\delta^{18}O$ vs. Cl^- plots (cfr. Fancelli & Nuti 1978; Perello et al. 2001). At Vinadio, these authors documented the presence of two chemical end-members, a low-salinity Na-SO_4-type, and a high-salinity Na-Cl-type. These two end-members occur in thermal waters, discharging a few metres away from a damage zone located at the borders of the Bersezio Fault Zone. The different Na^+ vs. Cl^- contents of the two end-members reflect a different content of the two components in the rocks within which they circulated. As an hypothesis, Perello et al. (2001) state that the low-salinity Na-SO_4-type waters originate from leaching of unaltered portions of granitic and migmatitic rocks, whereas the high-salinity Na-Cl-type waters originate from leaching of cataclastic hydrothermalized rocks, rich in phyllosilicate minerals and saline fluid inclusions.

Another factor influencing the hydraulic properties of fault rocks is the relative distribution of fracture intensity across the different lithologies. The fracturing of large rock volumes within granites allows pervasive diffuse fluid flow, whereas the localized fracturing within the migmatitic gneisses on the borders of the main fault zones leads to focussed fluid flow. Owing to these hydraulic properties, the granites at depth, below the migmatites (cfr. Fig. 15c) in the Vinadio and Valdieri sectors, are likely to represent large geothermal reservoirs for diffuse fluid flow with impervious boundaries constituted by the fan-shaped cataclastic faults. These combined factors may provide the favourable conditions for the development of deep and diffuse thermal circulations and the local up-well of thermal springs with temperatures close to 70 °C and flow rates up to 50 kg/s (Baietto 2007). According to Perello et al. (2001), meteoric waters infiltrate through the massif and, driven by topographic gradients, percolate to depths of 5–6 km where they attain temperatures up to ca. 150 °C (assuming gradients of 30–25 °C/km) and finally up-flow at valley bottoms. However, a buoyancy-driven flow ("free convection") also occurring within the high-permeability fracture zones of the granites is to be considered as a possible mechanism interacting with the topography-driven flow ("forced convection"). While forced convection refers to a flow driven by gravity, free convection refers to heat transfer in response to flow driven by temperature-induced density differences (Raffensperger & Vlassopoulos 1999). The potential for free convection is often investigated using the dimensionless Rayleigh number, which is derived from the ratio of buoyant and viscous forces. Theoretically, the onset of free convection in an infinitely extensive horizontal layer occurs when the Rayleigh number exceeds $4\pi^2$ (Lapwood 1948). This can occur for high values of the system permeability and/or for strong temperature gradients across the domain. However, there are limitations in applying the concept of the Rayleigh number to geometries more complex than a simple rectangularly shaped domain and in cases where the system is also perturbed by forced convection (Sorey et al. 1978). Some numerical modelling studies were aimed at exploring the conditions under which topography-driven and buoyancy-driven flow can coexist, giving rise to the so-called "mixed convection" (Forster & Smith 1988; López & Smith 1995; Raffensperger & Garven 1995; Thornton & Wilson 2007). These models have shown that free convection can develop in permeable zones if forced convection rates are limited by a low topographic gradient or if low-permeability layers isolate the buoyancy-driven flow from overlying topography-driven flow. Despite topography-driven flow is commonly assumed to overpower buoyancy-driven flow in mountainous regions, the existence of the latter condition seems to apply to Vina-

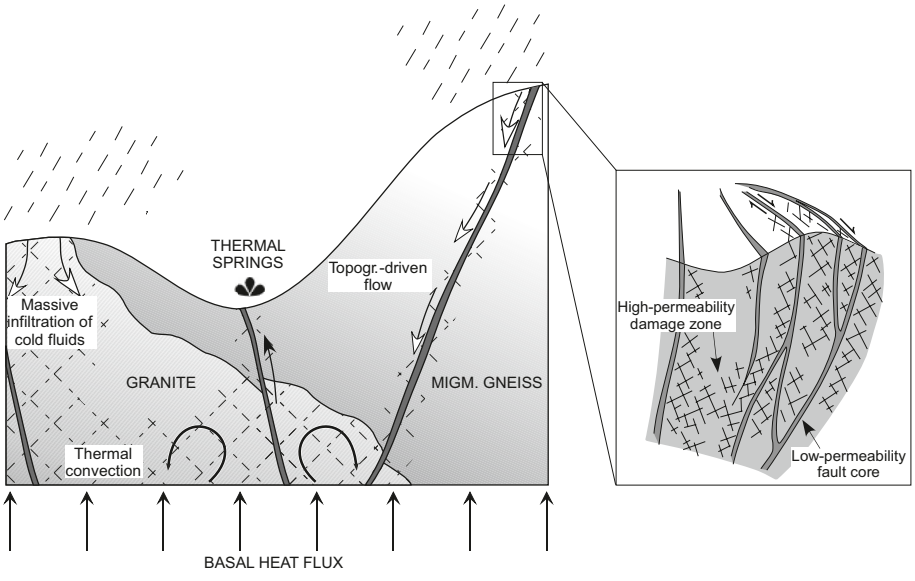

Fig. 16. Sketch depicting the thermal circulation patterns in the sectors of Bagni di Vinadio and Terme di Valdieri. Thermal convection onsets within granites in sites where the occurrence on top of migmatitic gneisses prevents the massive infiltration of cold waters from the surface. The inset on the right represents the complex system of conduits and barriers that characterize the cataclastic fault zones of Vinadio and Valdieri.

dio and Valdieri. In fact, the less fractured migmatitic gneisses sited above the more fractured granites can prevent massive infiltrations of cold meteoric waters, potentially favouring the onset of thermal convection inside the granites. Three-dimensional numerical simulations of the thermo-hydraulic flow at Valdieri further support the hypothesis of a mixed convection (Baietto *et al*. 2008). In fact, these models have shown that buoyancy-driven flow coexisting with topography-driven flow are a requirement for reconciling the numerical outputs with the water temperatures measured at the Valdieri springs. Buoyancy-driven circulation onsets at fault permeabilities exceeding 1×10^{-13} m^2, which is a value consistent with the permeabilities ($>1 \times 10^{-14}$ m^2) of the Bersezio Fault Zone, hydraulically similar to the faults feeding the Valdieri springs. Moreover, the simulations show that the existence of a high-permeability step-over zone at Valdieri is a factor that promotes the onset of a vigorous free convection, which would be much less effective along a single permeable fault zone. The numerical outputs indicate that the temperatures and discharge rates observed at Valdieri can be attained after 1500 years, assuming initial steady-state flow conditions.

The existence of mixed convection in the Alps is a rather new concept, since in this context the active thermal circulations have always been attributed to topography-driven flows only (Vuataz 1982; Rybach 1995; Perello 1997; Martinotti et al. 1999; Pastorelli et al. 1999; Pastorelli et al., 2001; Perello et al. 2001). Besides, it is possible that this mechanism could be at the origin of other high-temperature alpine spring systems and therefore its existence should be tested when hydrogeological investigations are performed.

6. Conclusions

This study investigated the relationships between the late-Alpine tectonic evolution of the Argentera Massif (Western Alps) and its fault-related thermal circulations at the sites of Bagni di Vinadio, Terme di Valdieri and Berthemont-Les-Bains. From the Early Miocene, the massif started its final uplift and experienced a protracted deformation under viscous, frictional-to-viscous and frictional conditions with the development of complex assemblages of structures and associated fault rocks. Deformations in viscous conditions yielded a mylonitic deformation along the Bersezio Fault Zone and the Fremamorta Shear Zone. These zones accommodated regional transpression and also constituted main pathways for fluid flow, promoting pervasive mineral reactions in lower greenschist facies conditions. Deformations occurring at frictional–viscous transition affected all the examined sectors and resulted in the development of diffuse slickensides, accompanied by a regional pervasive flow of meso-thermal fluids. During this phase, the massif recorded contrasting tectonic behaviour in its central and western part, the former being affected by transpression (despite strain partitioning also bringing about local transtension) and the latter by extensional tectonics. The orogen-parallel direction of extension in the Berthemont area seems consistent with a lateral extrusion provoked by the opening of the Ligurian Sea. This could have occurred during the Late Miocene, probably in a period during which the internal margin of the Argentera Massif was still recording a transpressive regime of crustal thickening. Deformation in frictional conditions brought about the development of regional systems of strike-slip cataclastic-gouge fault zones, mainly NW–SE and with a right-lateral shear sense. During this phase, both the central and western parts of the massif underwent transpressive wrench faulting under a NNE/NE direction of shortening. In the Vinadio and Valdieri sectors, the main faults form interconnected or en-échelon sets that are arranged in regional flower structures. The active geothermal reservoirs are hosted in between these structures. The patterns of thermal circulations within these reservoirs, including the infiltration of meteoric waters and the thermal discharges are mainly controlled by: (i) the geometrical features and by the relative proportion of low-permeability fault core (i.e. gouge and cataclasites) and high-permeability damage zones (i.e. fault breccia and fractures) of the cataclastic faults, (ii) the rheological response of the granites and the migmatites to the frictional deformation. The Vinadio and Valdieri faults can be viewed as complex systems of conduit-barriers while those of Berthemont behave mainly as conduit systems. At Vinadio and Valdieri, the hot springs occur in regions of fault interaction (respectively, in zones of extensional and contractional step-over) between two main NW–SE faults, while the Berthemont springs discharge close to a zone of fault intersection. Granites, which deform mainly by fracturing, are more suitable to host diffuse circulation, while migmatites, which deform either by cataclasis and fracturing, are more likely to act as combined conduit-barriers for fluid flow. It is proposed that deep-sited granites can constitute highly transmissive geothermal reservoirs. The occurrence at Vinadio and Valdieri of granites sited beneath migmatites seems a very favourable condition for the onset of buoyancy-driven circulations which combine with topograpy-driven flows, giving rise to a mixed convection. This is a reasonable explanation for the anomalously high temperatures that are observed at the Argentera hot springs and could presumably apply to other circulation systems in the Alps where high discharge temperatures are involved.

REFERENCES

Baietto, A. 2007: Fault-related thermal circulations in the Argentera Massif (South-Western Alps). PhD Thesis, Earth Science Department, University of Turin, 211 pp.

Baietto, A., Cadoppi, P., Martinotti, G., Perello, P., F.-D. Vuataz, Perrochet, P. 2008: Assessment of thermal circulations in strike-slip fault systems: the Terme di Valdieri case (Italian Western Alps). In: Wibberley, C. A. J., Kurz, W., Imber, J., Holdsworth, R. E. & Collettini, C. (Eds): The Internal Structure of Fault Zones: Implications for Mechanical and Fluid-Flow Properties, Geological Society Special Publication 299, 317–339.

Bigot-Cormier, F., Poupeau, G. & Sosson, M. 2000: Dénudation différentielles du massif cristallin externe alpin de l'Argentera (Sud-Est de la France) révélées par thermochronologie traces de fission (apatites, zir-

cons). Académie des Sciences de Paris, Earth and Planetary Sciences 330, 363–370.
Bogdanoff, S. 1986: Evolution de la partie occidentale du Massif cristallin externe de l'Argentera. Place dans l'arc Alpin. Géologie de France 4, 433–453.
Bogdanoff, S., Michard, A., Mansour, M. & Poupeau, G. 2000: Apatite fission track analysis in the Argentera massif: evidence of contrasting denudation rates in the External Crystalline Massifs of the Western Alps. Terra Nova 12, 117–125.
Bortolami, G. & Grasso, F. 1969: Osservazioni geologico-applicative sul cunicolo d'assaggio del traforo del Ciriegia e considerazioni sull'intero tracciato. Procedures of I International Congress: "Problemi tecnici nella costruzione di gallerie", 111–126.
Caine, J.S., Evans, J.P. & Forster, C. B. 1996: Fault zone architecture and permeability structure. Geology 24, 1025–1028.
Campredon, R. & Giannerini, G. 1982: Le synclinal de Saint Antonin (arc de Castellane, chaînes subalpines méridionales). Un exemple de bassin soumis à une déformation compressive permanente depuis l'Eocène supérieur. Géologie Alpine 58, 15–20.
Cevales, G. 1961: Il giacimento piombo-zincifero di Ruà presso le Terme di Vinadio, Valle Stura di Demonte, Cuneo. L'Industria Mineraria 12, 677–684.
Colomba, L. 1904: Cenni preliminary sui minerali del Lausetto (Valli del Gesso). Bollettino della Società Geologica Italiana 23, 392–397.
Compagnoni, R., Lombardo, B. & Prato, R. 1974: Andalousite et sillimanite aux contacts du granite central de l'Argentera (Alpes Maritimes), Società Italiana di Mineralogia e Petrologia 30, 1, 35–54.
Corsini, M., Ruffet, G. & Caby, R. 2004: Alpine and late-hercynian geochronological constraints in the Argentera Massif (Western Alps). Eclogae Geologicae Helvetiae 97, 3–15.
CNR 1990: Structural Model of Italy – Scale 1: 500000, Rome.
Curewitz, D. & Karson, J. 1997: Structural settings of hydrothermal outflow: Fracture permeability maintained by fault propagation and interaction. Journal of Volcanology and Geothermal Research 79, 149–168.
Dallmeyer, R. D. & Liotta, D. 1998: Extension, uplift of rocks and cooling ages in thinned crustal provinces: the Larderello geothermal area (inner Northern Apennines, Italy). Geological Magazine 135, 193–202.
Darcy, J. 1997: La nouvelle liaison routiere Nice-Cuneo et le Tunnel du Mercantour, Tunnels et ouvrages souterrains 139, 46–50.
Dewey, J. F., Holdsworth, R. E. & Strachan, R. A. 1998: Transpression and transtension zones. In: Holdsworth, R. E., Strachan, R. A. & Dewey, J. F. (Eds.): Continental Transpressional and transtensional Tectonics. Geological Society of London Special Publications 135, 1–14.
Evans, J.P., Forster, C.B. & Goddard J.V. 1997: Permeability of fault-related rocks, and implications for hydraulic structure of fault zones. Journal of Structural Geology 19, 11, 1393–1404.
Facello, A. 2006: Studio petrografico e microtermometrico delle inclusioni fluide nel giacimento idrotermale a Pb-Zn-fluorite di Ruà (vallone dei Bagni di Vinadio, Massiccio dell'Argentera). Thesis, Earth Science Department, University of Turin, 140 pp.
Fancelli, R. & Nuti, S. 1978: Studio geochimico delle sorgenti termali del Massiccio Cristallino dell'Argentera (Alpi Marittime). Bollettino della Società Geologica Italiana 97, 115–130.
Faulkner, D.R., Lewis, A.C. & Rutter, E.H. 2003: On the internal structure and mechanics of large strike-slip fault zone: field observations of the Carboneras fault in southeastern Spain, Tectonophysics 367, 235–251.
Faure-Muret, A. 1955: Etudes géologiques sur le massif de l'Argentera. Boillot, G. (Eds.): Les Marges continentales actuelles et fossiles autour de la Mercantour et ses enveloppes sédimentaires. Mémoires pour servir à l'explication de la carte géologique détaillé de la France. Paris: Imprimerie Nationale, 336 pp.
Ferrara, G. & Malaroda, R., 1969: Radiometric age of granitic rocks from the Argentera Massif (Maritime Alps). Bollettino della Società Geologica Italiana 88, 311–320.
Ford, M., Lickorish, W. H. & Kusznir 1999: Tertiary foreland sedimentation in the Southern Subalpine Chains, SE France: a geodynamic appraisal, Basin research 11, 315–336.
Forster, C. & Smith, L. 1988: Groundwater flow systems in mountainous terrain, 1, Numerical modelling technique. Water Resources Research 24, 999–1010.
Fry, N. 1989: South-westward thrusting and tectonics of the western Alps. In: Coward, M., Dietrich, D., Park, R. G. (Eds.): Alpine Tectonics. Geological Society of London Special Publications 45, 83–111.
Guardia, P., Ivaldi, J-P., Dubar M., Guglielmi, Y. & Perez, J.-L. 1996: Paléotectonique linéamentaire et tectonique active des Alpes maritimes franco-italiennes: une synthèse. Géologie de France 1, 43–55.
Hancock, P. L. 1985: Brittle microtectonics: principles and practice. Journal of Structural Geology 7, 437–457.
Harland, W. B. 1971: Tectonic transpression in Caledonian Spitzbergen, Geological magazine 108, 27–42.
Hirth, G., & Tullis, J. 1994: The brittle-plastic transition in experimentally deformed quartz aggregates, Journal of Geophysical Research 99, B6, 11, 731–11,748.
Holdsworth, R. E. 2004: Weak faults-rotten cores. Science 303, 181–182.
Horrenberger, J. C., Michard, A. & Werner, P. 1978: Le couloir de décrochement de Bersezio en Haute-Stura, Alpes externes, (Italie), structure de compression sub-méridienne. Sciences Géologiques Bulletin 31, 15–20.
Hubbard, M. & Mancktelow, N. S. 1992: Lateral displacement during Neogene convergence in the western and central Alps. Geology 20, 943–946.
Kamb, W. B. 1959: Ice Petrofabric Observations from Blue Glacier, Washington, in Relation to Theory and Experiment. Journal of Geophysical Research 64, 1891–1909.
Kerckhove, C. 1969: La "zone du Flysch" dans les nappes d'Embrunais- Ubaye. Géologie Alpine 45, 5–204.
Labaume, P., Ritz, J.-F. & Philip, H. 1989: Failles normales récentes dans les Alpes sud-occidentales: leurs relations avec la tectonique compressive. Comptes Rendus de l'Académie des Sciences de Paris II 308, 1553–1560.
Lapwood, E.R: 1948. Convection of fluids in porous medium. Proceedings of the Cambridge Philosophical Society 44, 508–521.
Larroque, C., Béthoux, N., Calais, E., Courboulex, F., Deschamps, A., Déverchère, J., Stéphan, J.-F., Ritz, J.-F. & Gilli, E. 2001: Active and recent deformation at the Southern Alps-Ligurian basin junction. Geologie en Mijnbouw 80, 255–272.
Latouche, L. & Bogdanoff, S. 1987: Evolution précoce du Massif de l'Argentera: apport des éclogites et des granulites. Géologie Alpine 63, 151–164.
Laubscher, H. 1991: The arc of the Western Alps today. Eclogae Geologicae Helvetiae 84, 631–659.
Laurent, O., Stephan, J.-F., Popoff, M. 2000: Modalités de la structuration miocène de la branche sud de l'arc de Castellane (chaînes subalpines méridionales). Géologie de France 3, 33–65.
López, D.L. & Smith, L. 1995: Fluid flow in fault zones: Analysis of the interplay of convective circulation and topographically driven groundwater flow. Water Resources Research 31, 6, 1489–1503.
Malaroda, R., Carraro, F., Dal Piaz, G.V., Franceschetti, B., Sturani, C. & Zanella, E. 1970: Carta geologica del Massiccio dell'Argentera alla scala 1:50.000 e note illustrative. Memorie della Società Geologica Italiana 9, 557–663.
Malaroda R., 1999: L'Argentera meridionale – Memoria Illustrativa della «Geological Map of the southern Argentera Massif (Maritime Alps) 1: 25.000». Memorie della Società Geologica di Padova 51, 91 pp., 156 ff., 1 carta geologica.
Marini, L., Bonaria, V., Guidi, M., Hunziker, J. C., Ottonello, G., Vetuschi, Zuccolini, M. 2000: Fluid geochemistry of the Acqui Terme-Visone geothermal area (Piemonte, Italy). Applied Geochemistry 15, 917–935.
Martinotti, G., Marini, L., Hunziker, J. C., Perello, P. & Pastorelli, S. 1999: Geochemical and geothermal study of springs in the Ossola-Simplon Region. Eclogae Geologicae Helvetiae 92, 295–305.
Merle, O. & Brun, J. P. 1984: The curved translation path of the Parpaillon Nappe (French Alps). Journal of Structural Geology 6, 711–719.
Michard, G., Grimaud, D., D'Amore, F. & Fancelli, R. 1989: Influence of mobile ion concentrations on the chemical composition of geothermal waters in granitic areas, example of hot springs from Piemonte (Italy). Geothermics 18 (5/6), 729–741.

Mugnier, J. L., Guellec, S., Menard, G., Roure, F., Tardy, M. & Vialon, P. 1990: Crustal balanced cross-sections through the external Alps deduced from ECORS profile. In: Heitzman, P., Roure, F. & Polino, R. (Eds.): Deep structure of the Alps. Mémoires Societé Géologique France 156, 203–216.

Musumeci G., Colombo F., 2002: Late Visean mylonitic granitoids in the Argentera Massif (Western Alps): age and kinematic constraints on the Ferrière-Mollières shear zone. Comptes Rendus de l'Académie des Sciences Serie II 334, 213–220.

Pastorelli, S., Marini, L. & Hunziker, J. C. 1999: Water chemistry and isotope composition of the Acquarossa thermal system, Ticino, Switzerland. Geothermics 28, 75–93.

Pastorelli, S., Marini, L. & Hunziker J. C. 2001: Chemistry, isotope values (δD, $\delta^{18}O$, $\delta^{34}S_{SO4}$) and temperatures of the water inflows in two Gotthard tunnels, Swiss Alps. Applied Geochemistry 16, 633–649.

Perello, P. 1997: Interazioni tra strutture tettoniche, fenomeni di sollevamento rapido recente e emanifestazioni geotermiche a bassa entalpia nelle Alpi occidentali. Studio di quattro località tipo: Settore Ossolano, Alta Valle d'Aosta, Settore Vallesano, Massiccio dell'Argentera. PhD Thesis, Earth Science Department, University of Turin.

Perello, P., Marini, L., Martinotti, G. & Hunziker, J. C. 2001: The thermal circuits of the Argentera Massif (western Alps, Italy): An example of low-enthalpy geothermal resources controlled by Neogene alpine tectonics. Eclogae Geologicae Helvetiae 94, 75–94.

Quintanilla., M. A. L., Suarez, V. F. 1996: Cerro Prieto and its relation to the Gulf of California spreading centres. Ciencias Marinas 22, 91–110.

Raffensperger, J.P. & Garven, G. 1995: The formation of unconformity-type uranium ore deposits: Coupled hydrochemical modeling, American Journal of Science 295, 639–696.

Raffensperger, J. & Vlassopoulos, D. 1999: The potential for free and mixed convection in sedimentary basins. Hydrogeology Journal 7, 505–520.

Romain, J. 1985: Données nouvelles sur l'environnement géologique des sources thermominérales de Berthemont-Les-Bains (Massif de l'Argentera-Mercantour, Alpes-Maritimes). Extrait des Actes du 110ème Congrès National Societé Savantes-Montpellier, 1985.

Rowland, J. V. & Sibson, R. H. 2004: Structural controls on hydrothermal flow in a segmented rift system, Taupo Volcanic Zone, New Zealand. Geofluids 4 (4), 259–283.

Rubatto, D., Schaltegger, U., Lombardo, B., Colombo, F. & Compagnoni, R. 2001: Complex Paleozoic magmatic and metamorphic evolution in the Argentera Massif (Western Alps) resolved with U–Pb dating, Schweizerische Mineralogische und Petrographische Mitteilungen 81, 213–228.

Rybach, L. 1995: Thermal waters in deep Alpine tunnels. Geothermics 24, 631–637.

Sanders, C. O., Ponko, S. C., Nixon, L. D. & Schwartz, E. A. 1995: Seismological evidence for magmatic and hydrothermal structure in Long Valley Caldera from local earthquake attenuation and velocity tomography. Journal of Geophysical Research 100, 5, 8311–26.

Schmid, S. M. & Handy, M. R. 1991: Towards a genetic classification of fault rocks: geological usage and tectonophysical implications. In: Muller, D. W., McKenzie, J. A. & Weissert, H. Eds. Controversies in modern geology, Academic Press 339–361.

Schmid, S. M., Fügenschuh, B., Kissling, E. & Schuster, R. 2004. Tectonic map and overall architecture of the Alpine orogen. Eclogae Geologicae Helvetiae 97, 93–117.

Scholz, C. H. & Anders, M. H. 1994: The permeability of faults. In: Hickman, Sibson, Bruhn The Mechanical Involvement of Fluids in Faulting (Eds): USGS Red Book LXIII, 247–253.

Segall, P. & Pollard, D.D. 1980: Mechanics of discontinuous faults. Journal of Geophysical Research 85, 4337–4350.

Seward, D. & Mancktelov, N. S. 1994: Neogene kinematics of the Central and Western Alps – Evidence from fission-track dating. Geology 22, 803–806.

Seward, D., Ford, M., Williams, E.A., Meckel, L.D. III & Bürgisser, J. 1999: Preliminary report on fission track studies in the Pelvoux area, SE France. In: G. Gosso, F. Jadoul, M. Sella & M. I. Spalla. 3rd Workshop on Alpine Geological Studies, Memorie della Società Geolologica (Padova University), 51, 1.25–32.

Sibson, R. H. 1977: Fault rocks and fault mechanisms. Journal of the Geological Society of London 133, 191–213.

Sibson, R. H. 1987: Earthquake rupturing as a mineralising agent in hydrothermal systems. Geology 15, 701–704.

Snoke, A. W., Tullis, J. & Todd, V. R. 1998: Fault-related rocks: a photographic atlas. Princeton University Press, 617 pp.

Sorey, M. L., Lewis, R. E. & Olmsted, F. H. 1978. The hydrothermal system of Long Valley caldera, California, U.S. Geological Survey Professional Paper 1044-A, A1-A60, 1978.

Steck, A. & Hunziker, J. 1994: The Tertiary structural and thermal evolution of the Central Alps—compressional and extensional structures in an orogenic belt. Tectonophysics 238, 229–254.

Stone, D. S. 1995: Structure and kinematic genesis of the Quealy wrench duplex: transpressional reactivation of the Precambrian Cheyenne belt in the Laramie basin, Wyoming. AAPG Bulletin 79, 1349–1376.

Sturani, C. 1962: Il complesso sedimentario autoctono all' estremo nord-occidentale des Massicio dell' Argentera (Alpi Marittime). Memorie dell'Istituto di Geologia e Mineralogia dell'Università di Padova 22, 178 pp.

Sue, C. & Tricart, P. 2003: Neogene to ongoing normal faulting in the inner western Alps: A major evolution of the late alpine tectonics. Tectonics 22,5–25.

Sue, C., Delacou, B., Champagnac, J.-D., Allanic, C., Tricart, P. & Burkhard, M. 2007: Extensional neotectonics around the bend of the Western/Central Alps: an overview. International Journal of Earth Sciences 96, 1101–1129.

Thorton, M.M. & Wilson, A. M. 2007: Topography-driven flow versus buoyancy-driven flow in the U.S. mid-continent: implications for the residence time of brines. Geofluids 7, 69–78.

Tricart, P. 2004: From extension to transpression during the final exhumation of the Pelvoux and Argentera massifs, Western Alps. Eclogae Geologicae Helvetiae 97, 429–439.

Tricart, P., Lardeaux, J-M., Schwartz, S. & Sue, C. 2006: The late extension in the inner western Alps: a synthesis along the south-Pelvoux transect. Bulletin de la Societe Géologique de France 177, 299–310.

Tullis, J. & Yund, R. A. 1977: Experimental deformation of dry westerly granite. Journal of Geophysical Research 82, B36, 5705–5718.

Vernet, J. 1965: Sur un décrochement horizontal tardif du socle dans la région méridionale de la zone des massifs cristallins externes (massif de l'Argentera, Alpes-Maritimes). Comptes Rendus de l'Académie des Sciences de Paris 258, 1358–1360.

Vuataz, F.-D. 1982: Hydrogéologie, géochimie et géothermie des eaux thermals de Suisse et des regions alpines limitrophes. Matériaux pour la Géologie de la Suisse – Série Hydrogéologie, 29, 174 pp.

Manuscript received December 4, 2007
Revision accepted December 4, 2008
Published Online first May 7, 2009
Editorial Handling: Stefan Bucher